



## Quantifying vessel noise and acoustic habitat loss in marine soundscapes

B. Hendricks<sup>a,\*</sup>, M.K. Pine<sup>b,c</sup>, G. Baer<sup>d</sup>, M. Welton<sup>e</sup>, H.K. Symonds<sup>f</sup>, D.T. Dakin<sup>g</sup>,  
H.M. Alidina<sup>h</sup>, C.R. Picard<sup>i</sup>, J. Wray<sup>d</sup>

<sup>a</sup> SoundSpace Analytics, 2845 Penrith Ave, Cumberland VOR 1S0, British Columbia, Canada

<sup>b</sup> Ocean Acoustics Ltd., 12 Muritai Road, Auckland 0620, New Zealand

<sup>c</sup> Institute of Life and Earth Sciences, Heriot-Watt University, Edinburgh EH14 4AS, United Kingdom

<sup>d</sup> North Coast Cetacean Society, 26 Cottonwood Rd, Alert Bay, VON1A0, British Columbia, Canada

<sup>e</sup> Saturna Island Marine Research & Education Society, PO Box 117, 727 Trillium Trail, Saturna Island, VON2Y0, British Columbia, Canada

<sup>f</sup> Pacific Orca Society, PO Box 510, Alert Bay, VON1A0, British Columbia, Canada

<sup>g</sup> Sea to Shore Systems Ltd., 1036 Clarke Rd, Brentwood Bay, V8M 1C7, British Columbia, Canada

<sup>h</sup> WWF-Canada, Resilient Habitats Program, 259-560 Johnson St., Victoria V8W 3C6, British Columbia, Canada

<sup>i</sup> Gitga'at Oceans and Land Department, 455 Hayimiisaxaa Way, Hartley Bay, VOV1A0, British Columbia, Canada

### ARTICLE INFO

#### Keywords:

Noise pollution  
Vessel detector  
Marine mammals  
Marine ecosystem management  
Listening space reduction  
Soundscape analysis

### ABSTRACT

Quantifying underwater vessel noise in marine ecosystems is challenging, due to difficulties in accounting for small, not publicly tracked boats, creating a knowledge gap in marine management. We present a computationally efficient framework that detects all vessel noise in hydrophone recordings and quantifies associated excess noise levels as well as acoustic habitat loss, offering a cost-effective and replicable tool for assessing vessel noise effects on marine soundscapes. Applied to one year of acoustic data from five sites along the coast of British Columbia (BC), Canada, the detector achieved 96.4 % accuracy and was robust against varying levels of vessel traffic and weather conditions. Across sites, vessel noise impacts increased with proximity to urban centers. Following this trend, average annual vessel noise presence ranged between 24 % and 85 %, increasing the 500 Hz decade band by 1.0 dB to 6.4 dB across sites. The average year-round acoustic habitat loss for killer whales, expressed as the reduction of listening space in a 0.5–15 kHz communication band, ranged from 6.6 % to 46.9 %. Vessel noise impacts were generally higher during daylight hours and in the summer months. The results are the first comprehensive, empirical assessment of vessel presence and associated noise impacts for a regional ecosystem in BC.

### 1. Introduction

Underwater noise radiated from vessels is a chronic stressor to marine ecosystems with documented adverse effects on marine mammals and other aquatic organisms, including behavioral changes (e.g., Williams et al., 2014; Gomez et al., 2016; Blair et al., 2016; van der Knaap et al., 2022), stress responses (e.g., Wright et al., 2007; Rolland et al., 2012), and acoustic masking (e.g., Tennessen et al., 2024; Erbe et al., 2019; Holt et al., 2009; Clark et al., 2009; Popper and Hawkins, 2019).

Underwater radiated noise (URN) from vessels originates from propeller cavitation, engines, the drive train, water pumps, and generators (Arveson and Vendittis, 2000; Barlett and Wilson, 2002). Source levels

and characteristics of vessel noise depend on vessel type, speed, length, and draft (e.g., MacGillivray and De Jong, 2021). Broadband URN ranges from 140 dB for small pleasure craft (Barlett and Wilson, 2002) to 204 dB for commercial cargo ships (MacGillivray and De Jong, 2021; MacGillivray et al., 2023; McKenna et al., 2012; Veirs et al., 2016). Of this, a significant portion is radiated in the form of narrowband frequencies with the strongest tonal frequencies typically between 10 and 1000 Hz (Arveson and Vendittis, 2000; Alexandri and Diamant, 2024; Aslam et al., 2024; McKenna et al., 2012; Ross, 2013; Hildebrand, 2009; Erbe, 2013). Small boats produce strong narrowband noise mostly between 200 and 800 Hz (Barlett and Wilson, 2002; Erbe et al., 2016; Pollara et al., 2017; Aslam et al., 2024), and therefore generally at

\* Corresponding author.

E-mail addresses: [benhendricks@soundspace-analytics.ca](mailto:benhendricks@soundspace-analytics.ca) (B. Hendricks), [matt.pine@ocean-acoustics.com](mailto:matt.pine@ocean-acoustics.com) (M.K. Pine), [grace@bcwhales.org](mailto:grace@bcwhales.org) (G. Baer), [maureen.welton@simres.ca](mailto:maureen.welton@simres.ca) (M. Welton), [helena@orcalab.org](mailto:helena@orcalab.org) (H.K. Symonds), [tomdakin@seatoshoresystems.ca](mailto:tomdakin@seatoshoresystems.ca) (D.T. Dakin), [halidina@wwfcanada.org](mailto:halidina@wwfcanada.org) (H.M. Alidina), [chriscard@gitgaat.ca](mailto:chriscard@gitgaat.ca) (C.R. Picard), [janie@bcwhales.org](mailto:janie@bcwhales.org) (J. Wray).

<https://doi.org/10.1016/j.marpolbul.2025.118150>

Received 30 March 2025; Received in revised form 10 May 2025; Accepted 11 May 2025

Available online 9 June 2025

0025-326X/© 2025 The Authors. Published by Elsevier Ltd. This is an open access article under the CC BY license (<http://creativecommons.org/licenses/by/4.0/>).

higher frequencies than large commercial ships (e.g., MacGillivray et al., 2024). For shallow-water recordings, low-frequency vessel noise may not propagate as well as in deep water, and be masked by flow noise around stationary hydrophones. Some studies have, therefore, measured peak narrowband vessel noise levels primarily above 100 Hz (Alexandri and Diamant, 2024; Mattmüller et al., 2024). The URN from vessels has become the dominant source of anthropogenic underwater noise and has elevated long-term ocean noise levels in many regions by more than 10 dB above ambient over recent decades (ZoBell et al., 2024; McDonald et al., 2006). At the same time, noise impact on underwater soundscapes is expected to rise with increasing industrial and recreational vessel activity, especially in coastal, near-shore environments (Hildebrand, 2009; ZoBell et al., 2024). As a result, the impact of vessel noise on marine life is a major focus of research and management worldwide (Southall et al., 2019; Marotte et al., 2022; Slabbekoorn et al., 2010; Breeze et al., 2022; Tasker et al., 2010; Peng et al., 2015; Chou et al., 2021; IMO, 2023).

British Columbia (BC) is the westernmost province of Canada and has an extensive, fragmented coastline comprising over 6000 islands and spanning approximately 29,000 km when following its full contour along the Pacific Ocean. BC's coastal waters are seasonally used by multiple populations of toothed and baleen whales listed under Canada's Species at Risk Act and contain designated critical habitat for species such as killer whales (*Orcinus orca*), humpback whales (*Megaptera novaeangliae*), and fin whales (*Balaenoptera physalus*). The BC coast also hosts Canada's largest port (Vancouver) and the eighth-largest port (Prince Rupert), as well as multiple smaller industrial terminals. In recent years, marine vessel traffic was growing on a coast-wide scale and is projected to continue to grow as additional industrial projects are approved and implemented. Vessel noise impact on marine ecosystems is expected to rise as a consequence (Keen et al., 2022; Gaydos et al., 2015)<sup>1</sup>. The impact of vessel noise has therefore been a key focus of marine management at federal, provincial, and community levels (Thornton et al., 2022; Malinka et al., 2024; Gaydos et al., 2015). Many of the existing efforts to better understand vessel noise and its impact on marine ecosystems in BC are related to the endangered Southern Resident Killer Whales (SRKWs) within their critical habitat in the Salish Sea (e.g., Malinka et al., 2024; Burnham et al., 2021; Joy et al., 2019; Heise, 2008; Lacy et al., 2017; Burnham et al., 2023; MacGillivray et al., 2024). In contrast, the sparsely-populated regions along the North and Central Coast are poorly studied regarding vessel noise and its impacts on marine life.

The monitoring of marine vessel traffic is most commonly accomplished using AIS (Automatic Identification System) data, which also serves as the basis for the assessment of existing or projected vessel noise by means of noise modeling (see O'Hara et al., 2023, a review in Robards et al., 2016, or Erbe et al., 2012; MacGillivray et al., 2024; ZoBell et al., 2024). Vessel noise modeling requires a good understanding of the receiving environment and parameterization of it, as well as catalogued source levels for different vessel categories in combination with AIS data to reconstruct vessel traffic and noise. However, many smaller vessels do not carry AIS (referred to in this paper as non-AIS vessels) and their presence is otherwise not efficiently tracked by radar or visual imagery. As a result, models are effective in areas dominated by industrial shipping noise, but become inaccurate in regions where non-AIS vessels significantly contribute to the soundscape (Merchant et al., 2014; MacGillivray et al., 2024) or in regions with complex environmental conditions. In BC, non-AIS vessels constitute approximately 70–85 % of the total fleet in the South (O'Hara et al., 2023; Murphy et al., 2023) and seasonally between 50 and 80 % along BC's Northern Coast (*N. Serra-Sogas pers. com.*). Non-AIS vessels have been shown to increase long-term average sound levels in BC (Thornton et al., 2022) and elsewhere (Wilson et al., 2022), and recent models suggest that during parts of the

year non-AIS vessels are responsible for the majority of the total vessel noise budget in some frequency bands and areas within Southern BC (MacGillivray et al., 2024). Given that there is a potentially significant but not well quantified component of noise from non-AIS vessels in many regions, it is essential to account for these contributions in underwater noise monitoring and management efforts (Serra-Sogas et al., 2021; Pollara et al., 2017).

Acoustic detection of vessel noise can capture all vessel types over large ranges and in recent years detection of vessel noise in passive acoustic monitoring (PAM) surveys has seen an increase in designs and applications (Ji et al., 2024; Alexandri and Diamant, 2024; Kaplan and Mooney, 2015; Pollara et al., 2017; Reis et al., 2019; Simard et al., 2016; Merchant et al., 2014). However, many existing studies have been carried out only in controlled environments (Liu et al., 2024; Sorensen et al., 2010), are restricted to specific vessel types or noise patterns (Ji et al., 2024; Reis et al., 2019; Merchant et al., 2014), are limited in geographic scope (Reis et al., 2019), or have restricted temporal and seasonal coverage (Vieira et al., 2020; Kaplan and Mooney, 2015). Moreover, most detection frameworks do not quantify noise levels associated with marine vessels.

This study presents a computationally efficient framework for detecting vessel noise in underwater soundscapes. This framework provides the ability to quantify the contribution of vessel noise on ambient sound levels (expressed as excess noise of the natural soundscape), as well as the acoustic habitat loss for marine mammals (expressed as a reduction in available listening space). The detector's performance was assessed using five regional soundscapes in BC, for which annual vessel noise patterns and the listening space reduction for killer whales was determined to establish local baselines and tangible metrics for ongoing acoustic monitoring efforts within these ecosystems.

## 2. Methods

### 2.1. Acoustic data

All acoustic data for this study were collected by partners of the BC Hydrophone Network (BCHN).<sup>2</sup> The BCHN coordinates community-based acoustic monitoring efforts and produces long-term, standardized acoustic data from near-shore hydrophone sites for acoustic monitoring to establish and enhance marine ecosystem knowledge along the coast of BC. While individual data ownership is maintained, these datasets together constitute one of the three largest sources of acoustic data in BC (besides Ocean Networks Canada, and the federal Department of Fisheries and Oceans), providing extensive temporal and spatial coverage along the coast.

This study used data from five underwater acoustic recording sites across four broader regions (see Fig. 1): the Salish Sea (SS-1), Northern Vancouver Island (NI-1, NI-2), the Central Coast (CC-1), and the Northern Coast (NC-1). All deployment sites are located within known habitat for several at-risk cetacean species, including SRKWs (SS-1), Northern Resident killer whales (NRKWs; NI-1, NI-2, CC-1, NC-1), Bigg's killer whales (all sites), fin whales (NC-1), and humpback whales (all sites). SS-1 was located off East Saturna Island, facing Boundary Pass—a major commercial shipping corridor with over 7000 vessels transits annually to and from the Port of Vancouver (Erbe et al., 2012; Veirs and Veirs, 2005; Veirs et al., 2016) and located within critical habitat for SRKWs. SS-1 is owned and operated by the Saturna Island Marine Research and Education Society.<sup>3</sup> NI-1 and NI-2 were located near the northern end of Vancouver Island, facing Blackfish Sound (NI-1) and Johnstone Strait (NI-2). This area is an important traffic corridor known as the Alaskan Marine Highway for both commercial and recreational vessels traveling between Vancouver Island, the Northern Coast, and

<sup>1</sup> see also <https://www.rupertport.com/future-growth/>

<sup>2</sup> <https://whalesound.ca>

<sup>3</sup> <https://simres.ca>

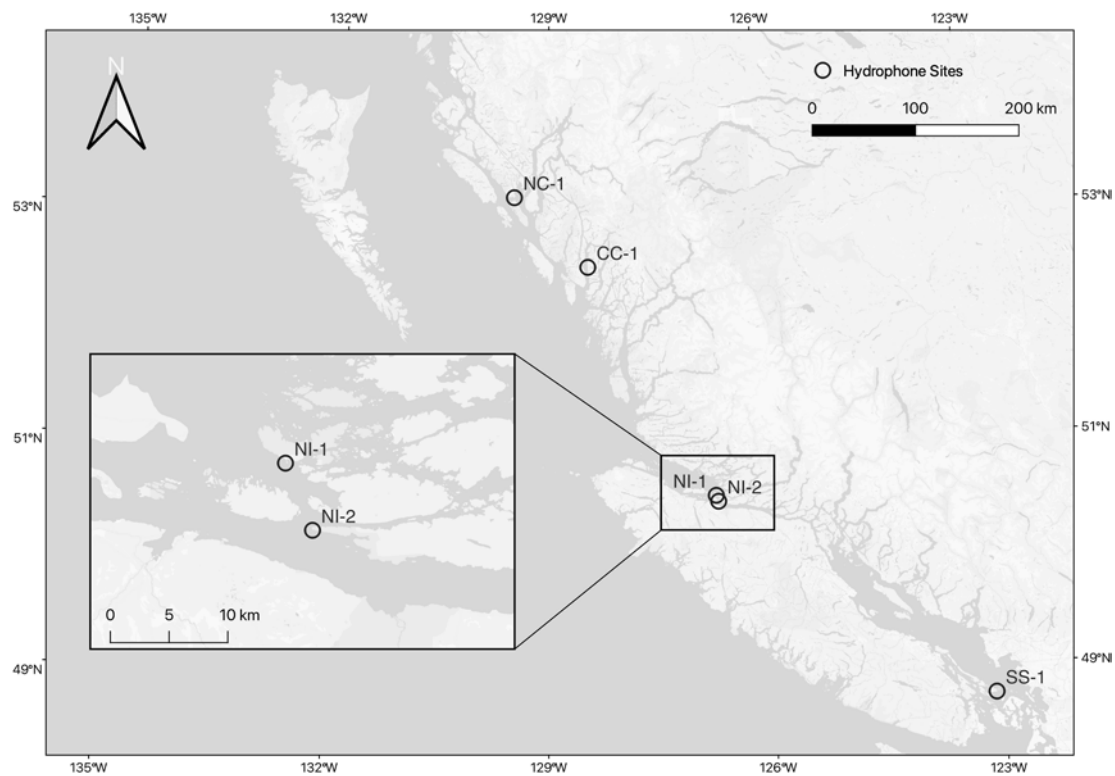


Fig. 1. Location of hydrophone sites along the coast of BC used in this study.

Alaska. It is also a major hub for vessel-based whale watching and nature viewing. The region is critical habitat for NRKWs and features the only permanent Killer Whale Marine Sanctuary in Canada, the Robson Bight (Michael Bigg) Ecological Reserve. NI-1 and NI-2 are owned and operated by OrcaLab.<sup>4</sup> CC-1 was located off Roderick Island in the Central Coast, facing Finlayson Channel, which is a northern section of the Alaskan Marine Highway. It is within the acoustic range of ferries docking at the BC Ferries terminal in Klemtu in Kitasoo Xai'xais Territory. CC-1 is owned and operated by the Kitasoo Xai'xais Nation.<sup>5</sup> NC-1 was located off Pitt Island on the North Coast, facing Squally Channel, located within a recently commissioned LNG shipping corridor to and from Kitimat. Squally Channel is within shortlisted critical habitat for several whale species, including fin whales, humpback whales, NRKWs, and Bigg's killer whales. NC-1 is owned and operated by the SWAG project (Ships Whales and Acoustics in Gitga'at Territory).<sup>6</sup>

Data were recorded at all sites using a standardized deployment design and storage protocol, using icListen HF hydrophones,<sup>7</sup> deployed in water depths of 20–40 m, on tripod moorings holding the hydrophone 70 cm above the seafloor. The moorings were cabled to a shore station providing power and GPS time synchronization. Data were logged in 300 s increments at 64 kHz, except for SS-1/Boundary Pass, which logged at 128 kHz. An anti-aliasing filter at 85 % of the Nyquist frequency yielded a high-frequency cut-off at approximately 27 kHz (54 kHz for SS-1). The deployment design allowed for continuous, long-term data collection that was only sporadically interrupted by power outages. Overall recording effort ranged from 91 % to 96 % across sites within the 12 month time periods listed in Table 1 (see Fig. 1-S in Supplemental Materials for details).

All hydrophones were high-frequency calibrated ( $\geq 10$  kHz) by the

manufacturer prior to deployment. Because low-frequency calibration was not available for individual units before deployment, the known low-frequency roll-off curves from 20 icListen HF units were averaged and applied to all units used in this study. Being part of the BCHN monitoring program, hydrophones at all sites were also deployed before and after the time windows chosen for this study and were re-calibrated every two years. The calibration drift over a two year deployment was  $< 2$  dB across the frequency spectrum.

Data from all hydrophone sites showed low-amplitude, single-frequency tonal spikes, associated with self-noise from the hydrophone (see Fig. 2-S in Supplemental Materials) with different models of icListen HF hydrophones showing slightly different tonal frequencies and amplitudes.

## 2.2. Processing framework

The vessel noise detection and quantification framework was organized into three steps (see Fig. 2):

1. Detection of vessel noise: a subset of the acoustic data was annotated to optimize and subsequently assess the vessel noise detection framework (Section 2.3). Acoustic time segments were classified as either *vessel noise* or *natural ambient*, based on the detected presence or absence of vessel noise (see Section 2.4).
2. Vessel excess noise levels: the rise in natural ambient levels due to vessel noise, expressed as the excess noise  $\Delta$ dB, was calculated by comparing reconstructed soundscapes with and without vessel noise (Section 2.5). An error analysis was conducted to quantify uncertainties associated with  $\Delta$ dB (Section 2.5.3).
3. Listening space reduction: results from vessel excess noise levels were used to compute the reduction of listening space for killer whales at all study sites (Section 2.6).

<sup>4</sup> <https://orcalab.org>

<sup>5</sup> <https://klemtu.com/>

<sup>6</sup> <https://www.swag-project.org/>

<sup>7</sup> <https://oceansonics.com/iclisten-hf-hydrophone>

**Table 1**  
Hydrophone locations and data collection summary.

Site ID	Geographic Name	Latitude N	Longitude W	Deployment Start	Deployment End
SS-1	Monarch Head	48°46'01.2"	123°05'27.6"	Jan 01, 2023	Dec 31, 2023
NI-1	Flower Island	50°36'00.0"	126°42'28.8"	Jan 01, 2023	Dec 31, 2023
NI-2	Cracroft Point	50°32'52.8"	126°40'40.8"	Jan 01, 2023	Dec 31, 2023
CC-1	Mary Cove	52°36'18.0"	128°26'34.8"	May 01, 2023	Apr 30, 2024
NC-1	Otter Channel	53°12'38.8"	129°29'55.0"	May 20, 2023	May 19, 2024

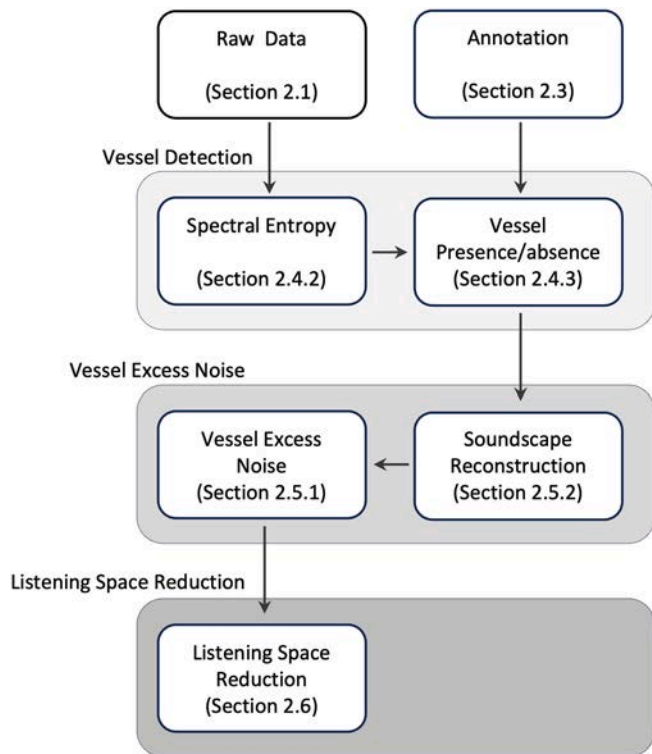


**Fig. 2.** Schematic of algorithm for vessel noise detection, and computation of excess noise and listening space.

All data processing, analyses and visualization were performed using the Python programming language,<sup>8</sup> and a modified version of the R package ‘soundcheck’ was used for data annotation.<sup>9</sup>

### 2.3. Data annotation

A subset of the data was manually annotated for the presence or absence of vessel noise to identify optimal parameters for the detection algorithm and to assess detector performance.

For each site, 35 recording segments of 60 s per day were randomly selected for three calendar days at the beginning, middle, and end of each calendar month. This approach ensured that all seasonal and diurnal conditions were equally sampled. In total, 5854 acoustic segments were annotated, equivalent to 1.2 % of each site’s analyzed data. A spectrogram (NFFT= $f_s$ , Hanning window, 50 % overlap) was generated with a logarithmically scaled frequency range from 50 Hz to 2 kHz. Each spectrogram was 300 s long and centered around the 60-second assessment segment to provide context for easier vessel signature identification. Segments were inspected aurally and visually for vessel noise and categorized as: (1) vessel noise present, (2) vessel noise absent, or (3) ambiguous. To assess objectivity in the annotation process, data from

one site (NI-2/Cracroft Point) were independently annotated by two inspectors. Segments labeled ambiguous were excluded from the annotation set, and the remaining annotated segments were used for optimization and performance assessment.

Detector performance was assessed using Precision ( $P$ ) & Recall ( $R$ ) as well as Accuracy ( $Acc$ ). Correctly identifying vessel noise presence was equally important to identifying the absence of vessel noise. Precision and Recall were therefore computed with respect to both these subsets (indicated as suffix 1 for presence and 0 for absence of vessels):

$$P_{1/0} = \frac{TP_{1/0}}{TP_{1/0} + FP_{1/0}} \quad (1)$$

and

$$R_{1/0} = \frac{TP_{1/0}}{TP_{1/0} + FN_{1/0}} \quad (2)$$

Accuracy was used to optimize detector performance as it takes into account both subsets:

$$Acc = \frac{TP_1 + TP_0}{TP_0 + TP_1 + FP_0 + FP_1} \quad (3)$$

In all equations,  $TP$ ,  $FP$ , and  $FN$  denote true positive, false positive, and false negative detections, respectively.

## 2.4. Vessel noise detection

### 2.4.1. Concept

Tonal signals are a ubiquitous component of the URN from any motorized vessels (Alexandri and Diamant, 2024; Pollara et al., 2017), and can even dominate the total radiated noise (Arveson and Vendittis, 2000). Previous studies have used the presence of these narrowband features to detect or classify vessel signatures (Reis et al., 2019; Pollara et al., 2017; Alexandri and Diamant, 2024; Siddagangaiah et al., 2016; Simard et al., 2016). In contrast, the signatures of natural sources such as wind, waves, etc. (i.e. geophony) lack narrowband spectral energy (Erbe and King, 2008) and create a high-entropy acoustic environment. Vessel noise suppresses this naturally high-entropy state, and we hypothesize that in most soundscapes, human-generated underwater noise is the only sustained low-entropy sound source.

The vessel noise detector presented here leverages this dichotomy in the entropy between vessel and natural sound. By assessing the spectral entropy in recorded underwater noise, the time segments with vessel or natural noise were identified. In underwater acoustics, entropy-based indices have been shown to correlate with the acoustic presence of vessels (Ferguson et al., 2023). Entropy has also been used to detect marine mammal calls (e.g., Erbe and King, 2008; Bougher et al., 2012; Hendricks et al., 2018) and to classify vessel types (e.g., Wang and Chen, 2019). Here, these concepts are synergized to form the central method for detecting and quantifying vessel noise.

### 2.4.2. Computing spectral entropy

Power spectral densities (PSD) were computed from hydrophone recordings with sampling rate  $f_s$  using a Fast Fourier Transform (FFT);

<sup>8</sup> Python Software Foundation, [python.org](https://python.org)

<sup>9</sup> <https://github.com/ericmkeen/soundcheck>

Hanning Window, 50 % overlap, NFFT =  $f_s$ ) to achieve a 1 Hz frequency resolution. The spectra were then averaged to 60-second segments using the median, which effectively removed transient biophonic signals.<sup>10</sup> Within the 60-second time window, most narrowband vessel signatures, including those from small boats, remained stable. Spectral entropy  $H(s)$  was then calculated for successive median 60-second PSDs ("spectra") in linear space, using the following steps:

1. The spectra were trimmed to a frequency range of 80–1000 Hz. The 80 Hz lower cut-off reduced the impact of flow noise and minimized contributions from wind and waves (Wenz, 1962; Merchant et al., 2014). While commercial ships emit high noise levels below 80 Hz, received narrowband levels recorded in shallow-water often peak above 100 Hz, due to a poorer propagation environment for these low-frequencies (e.g., Alexandri and Diamant, 2024; Barlett and Wilson, 2002; Mattmüller et al., 2024). This effect was also observed in our data where more than 98 % of the annotated segments with vessel noise contained signatures within the 80–1000 Hz detection window (see also Fig. 7). Additionally, the 80 Hz cut-off mitigates common hydrophone low frequency roll-off, while the 1 kHz cut-off helps exclude the majority of electrical self-noise (Fig. 2-S in Supplemental Materials).
2. Self-noise within the 80–1000 Hz band varied based on the model of hydrophone and power supply. To determine the affected frequency bands for each site, spectral probability densities (SPDs) were computed for monthly periods. Narrow-band spikes in the 1st percentile of these monthly SPDs were deemed system-related noise, and 5 Hz wide windows centered around those single-frequency tonals were excluded from the spectra.
3. The spectra were divided by a flattening function, defined as the median value over a 50 Hz rolling window centered symmetrically around each assessed value.
4. The spectra were normalized through division by the sum of its values, resulting in a function with the properties of a probability distribution.
5. The spectral entropy ( $H$ ) of the trimmed, flattened, and normalized 60-second spectra ( $s$ ) with  $N$  frequency elements was then calculated using Eq. 4. Here,  $H(s) = 0$  if  $s$  is highly ordered, and  $H(s) = 1$  if  $s$  is uniformly random:

$$H(s) = -\frac{1}{\log_{10}(N)} \sum_{k=1}^N S_k \log_{10}(S_k) \quad (4)$$

#### 2.4.3. Vessel presence

For all sites, the 60-second spectral entropy values exhibited a bimodal distribution: high-entropy ambient sound segments were separated from segments with low-entropy vessel noise. This pattern was consistent across all sites, irrespective of vessel noise intensity, prevailing ambient conditions, bio-acoustic activity, or vessel types present. The probability density distribution of spectral entropy is shown in relation to mean-square sound pressure levels (symbol  $L_p$  or sound levels) in a diagram for all sites in Fig. 3.

A binary decision for the presence or absence of vessels was made using a threshold ( $H_T$ ) applied to the spectral entropy  $H(s)_t$  for each 60 s acoustic recording segment  $t$ : Segments with  $H(s)_t \leq H_T$  were classified as vessel noise, time segments with  $H(s)_t > H_T$  were classified as natural ambient. The value of  $H_T$  was informed by the annotated dataset (see Section 2.3), and equal weight was given to correctly classifying both vessel noise and natural ambient segments.

Finally, spurious outliers were removed by first assigning natural ambient segments as vessel noise that were shorter than 120 s (i.e. 2

consecutive segments were needed to count as natural ambient), then assigning vessel detection segments as natural ambient if they did not form consecutive windows of at least 300 s (i.e. 5 consecutive segments were needed to count as vessel noise).

As a result, a binary decision with respect to the presence of vessel noise was assigned to all available 60-second time segments of recorded acoustic data (Fig. 7).

## 2.5. Vessel excess noise

### 2.5.1. Concept

The impact of vessel noise on the soundscape was assessed by quantifying the excess noise  $\Delta\text{dB}$  from vessels, defined as the arithmetic difference between the underlying natural ambient sound level  $L_p, \text{amb}(t, f)$  and the total sound level  $L_p, \text{tot}(t, f)$  for any given time segment  $t$  and frequency band of interest  $f$  (Eq. 5):

$$\Delta\text{dB}(t, f) = L_p, \text{tot}(t, f) - L_p, \text{amb}(t, f). \quad (5)$$

$L_p, \text{tot}(t, f)$  comprised all audio segments (i.e. those with vessel noise and those with natural ambient conditions) and formed a time sequence matching the available data. The natural ambient time sequence  $L_p, \text{amb}(t, f)$  was defined as the underlying ambient sound level if no vessel noise was present at any given moment (further described in Section 2.5.2 below). Finally,  $\Delta\text{dB}(t, f)$  is always positive, meaning that the presence of vessel noise always elevates the natural ambient level, and  $\Delta\text{dB}(t, f)$  is zero if no vessel noise is present for a given  $t$  and  $f$ .

This provided a measure of how much area-specific sound levels were elevated by URN from vessels at a high temporal resolution. Sound levels for Eq. 5 were computed from power spectra similar to those described in Section 2.4.2 with the exception that 60 s time segments were averaged in linear space using the mean.

Vessel excess noise levels presented in the main body of this manuscript were computed in dB re  $1\mu\text{Pa}$  for the frequency band of 80–1000 Hz used for the vessel detector, as well as in one-tenth decade (decidecade) bands (ISO 18405, Ainslie et al., 2022). Additionally, an Appendix lists seasonal vessel excess noise levels for all sites for octave frequency bands from 31.5 Hz to 16 kHz, as well as three decade bands (10–100 Hz, 100–1000 Hz, 1–10 kHz).

### 2.5.2. Reconstructing natural ambient sound levels

To determine how vessel noise increased natural ambient sound levels at each site, the natural ambient sound level without vessel noise ( $L_p, \text{amb}(t, f)$ ) was estimated. This reconstruction of the natural soundscape was done using the following steps:

- A consecutive time sequence of sound levels, with equally-spaced 60-second intervals, was constructed by indexing each  $L_p$  segment that did not contain vessel noise. Intervals that contained vessel noise or lacked recorded data were filled with NaN, creating 'gaps' in the time-series vector.
- Those gaps within the array were then replaced with linearly-interpolated values based on the edge values without vessel noise. This was done for all gaps up to 10 h. Gaps for which the time difference to the next known ambient  $L_p$  value was greater than 10 h were not replaced. This resulted in complete interpolation for vessel noise gaps shorter than 20 h and partial interpolation for longer gaps. The 10-hour threshold was a 'common-sense' estimate, balancing the reliability of inferring ambient levels with the need to bridge gaps of extended vessel noise presence. Interpolated ambient noise levels during periods of consecutive vessel noise exceeding 20 h were considered not reliable and were excluded from the excess noise analysis. The fraction of data that was excluded because of this was < 1%, with the exception of SS-1 where 9 % of segments were removed.
- For a few time segments, estimated natural ambient levels exceeded the corresponding levels in the anthropogenic time sequence. For

<sup>10</sup> of the 2616 segments annotated as natural ambient across sites, only 3 (0.1 %) were incorrectly classified as vessel noise because of the presence of marine mammal vocalizations.

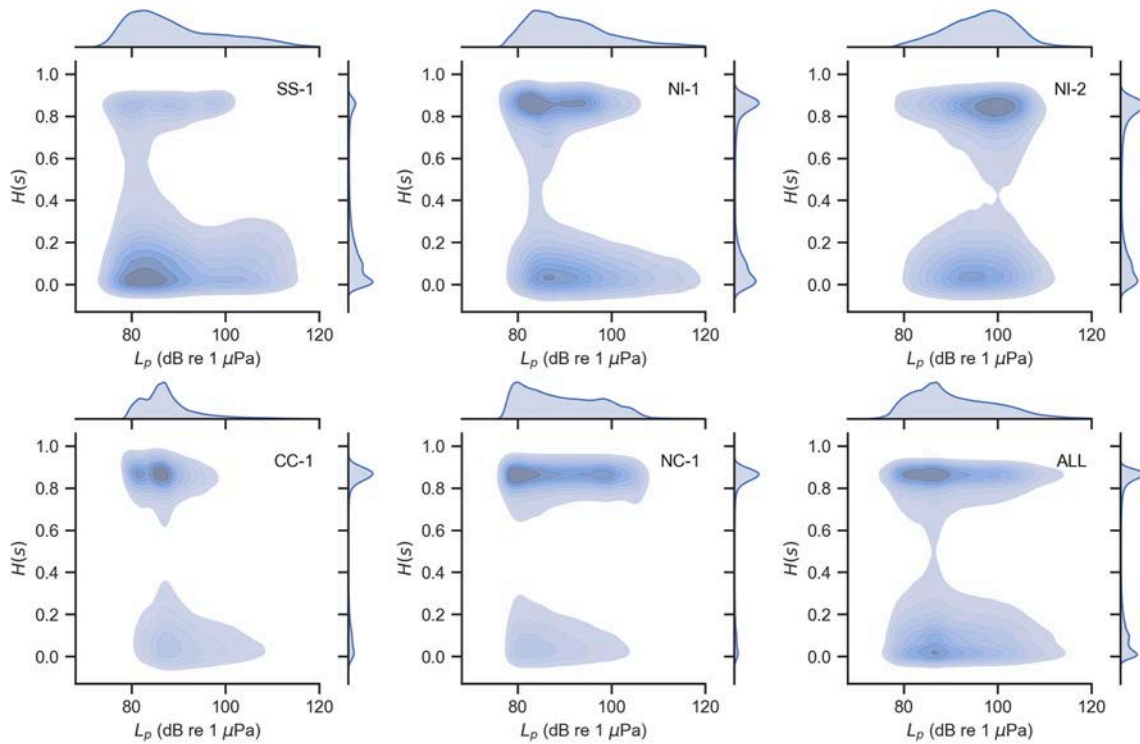


**Fig. 3.** Amplitude-Entropy diagrams for individual sites (SS-1, NI-1, NI-2, CC-1, NC-1) and the combined data (ALL). Shown are kernel density estimations for all available time segments (approximately 500,000 per site and 2.5 M for the combined data). All sets displayed a clear bimodal distribution in spectral entropy  $H(s)$  associated with the presence and absence of vessel noise. No such distribution was seen for recorded sound levels (here: 80–1000 Hz).

these intervals, values of the linear interpolation function were replaced with the lower convex hull (i.e., the lower envelope connecting the local minima within the interpolation window) of concurrent anthropogenic noise levels to ensure  $\Delta dB(t, f) \geq 0$  at all times (see Fig. 4, right panel). The correction effect was small with  $\Delta dB < 0.3$  dB on average over a full year across sites for  $f = 80 - 1000$  Hz.

- Finally, the reconstructed natural ambient sequence was trimmed to match the same time windows as  $L_{p,tot}(t, f)$  (Fig. 4).

2.5.3. Error analysis

The interpolation process described in Section 2.5.2 introduced a random error to  $L_{p,amb}(t, f)$  and subsequently to  $\Delta dB(f)$  for time-integrated periods. This error,  $\sigma[\Delta dB(f)]$ , was assessed using known time windows of natural ambient soundscape conditions (i.e. consecutive segments with absence of detected vessel noise). Those periods of natural ambient conditions were used to apply the same interpolation procedure that was used to reconstruct natural ambient sound levels during the presence of vessels (i.e. linearly connecting the start and end

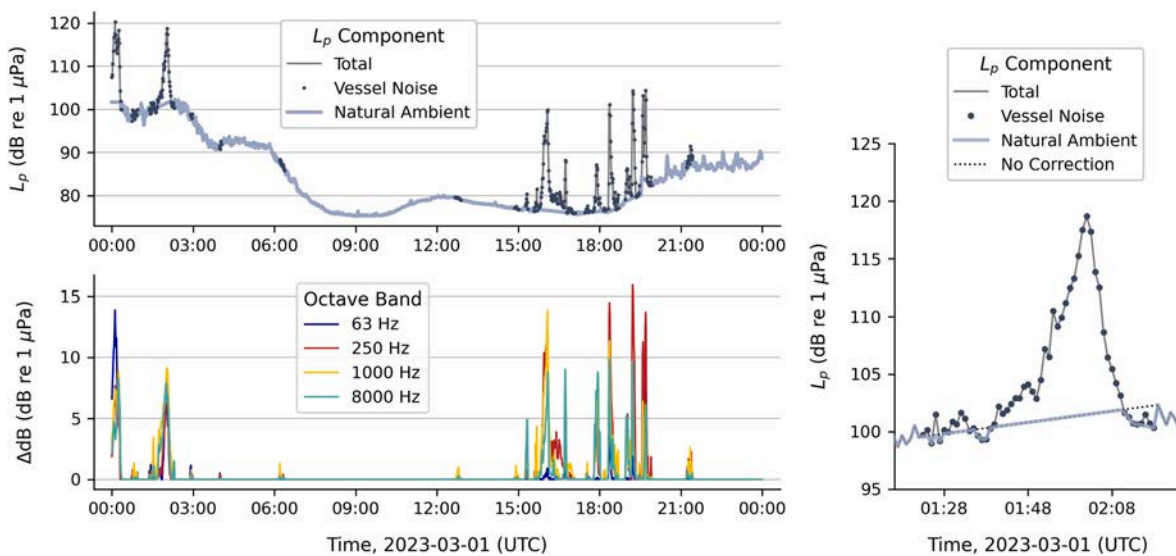


**Fig. 4.** Top left: construction of natural ambient time sequence  $L_{p,amb}(t, f)$ : segments with detected vessel noise (dots) are removed from the total sound level and the gaps are interpolated to the nearest natural ambient sound level. Levels are shown for the 80–1000 Hz frequency band. Bottom left:  $\Delta dB(f, t)$  for selected octave frequency bands. Right: application of a lower convex hull correction to adjust the interpolated natural ambient sequence to below the lowest measured sound levels within the interpolation range. All three graphs show data from the same day and site (NI-1/Flower Island; Mar 01, 2023).

points), except that here the true underlying natural ambient sound level was known. By comparing the true to the interpolated sound levels for each available window of set length  $t_{gap}$ , the expected  $\sigma[\Delta\text{dB}(f)]$  for an interpolation interval of length  $t_{gap}$  was then equal to the standard deviation of those individual differences (see Fig. 5).

The total error for  $\Delta\text{dB}(f)$  within the seasonal and diurnal categories was then estimated using Eq. 6:

$$\sigma[\Delta\text{dB}(f)] = \frac{p_{tot}}{n} \times \sigma[\Delta\text{dB}(f)_{ave}] \quad (6)$$

in which  $\sigma[\Delta\text{dB}(f)_{ave}]$  is  $\sigma[\Delta\text{dB}(f)]$  for the site-specific average interpolation length  $t_{ave}$ ,  $p_{tot}$  is the fraction of vessel noise presence, and  $n$  is the maximum number of  $t_{ave}$ -sized segments that fit in a seasonal or diurnal sequence.

## 2.6. Listening space reduction for killer whales

The elevation of ambient sound levels caused by vessel noise results in auditory masking in marine mammals and therefore in the degradation of their acoustic habitat. This impact of vessel noise can be quantified as listening space reduction (LSR), expressed as a percentage change from an original listening space available under natural ambient conditions (e.g., Pine et al., 2018). The frequency band for which LSR is computed can be specifically chosen to be relevant for a target species. Therefore, LSR provides an impact metric with relevance to marine managers and territorial stewards.

Here, LSR was computed for killer whales using a frequency band of 0.5–15 kHz, which has been established as a generalized communication band for this species (Heise et al., 2017). All sites in this study are known habitat for at least two of the three ecotypes that use coastal BC waters (SRKWs, NRKWs, Bigg's) and three sites (SS-1, NI-1, and NI-2) are designated critical killer whale habitat. LSR was computed using equations presented in Pine et al. (2018):

$$LSR = 100 \left( 1 - 10^{-\frac{2\Delta\text{dB}}{N}} \right) \quad (7)$$

In Eq. 7,  $\Delta\text{dB}$  is the vessel excess noise, or the difference between the natural ambient and the elevated sound level. Here,  $\Delta\text{dB}$  was obtained from Eq. 5 for all time windows.  $N$  is a scaling coefficient that characterizes the propagation loss. It is unique to local bathymetric features, water and seabed properties, and frequency (e.g., Pine et al., 2018). A standardized LSR was computed using  $N = 15$ , a typical value recommended to approximate propagation loss in near-shore environments.<sup>11</sup> Seasonal-diurnal LSR profiles were then derived for all sites by computing average LSR percentages from excess noise levels for each hour-of-day within all available data.

## 3. Results

### 3.1. Detector performance

A total of 5337 annotated acoustic segments (2616 natural ambient, 2721 with vessel noise) were used for optimization and performance assessment, after excluding ambiguous segments. The fraction of segments labeled as ambiguous was equally low for both inspectors (5.9 % and 7.5 %, respectively), as was the fraction of files containing vessel noise signatures only outside the detector's frequency window (2 % and 1.7 %, respectively). The two inspectors agreed on 99.3 % of the commonly inspected, non-ambiguous segments.

The best average allocation accuracy of the vessel noise detector was achieved with a threshold of  $H_T = 0.6$ . This threshold provided the best

average performance across sites, with an accuracy of 96.4 % (lowest: 93.8 %, highest: 97.9 %). Performance evaluation showed that the detector was robust within a wide range of anthropogenic, bionic, and environmental sound sources. Similar results were achieved for  $0.3 \leq H_T \leq 0.7$  and equally high detector accuracies were achieved with a single choice for all sites (see Fig. 6). The detection framework was therefore applied to all data using a universal threshold parameter of  $H_T = 0.6$  and without any other site-specific parameterization. The accuracy, precision, and recall statistics using this approach are summarized in Table 2 for each study site.

Fig. 7 shows a typical long-term spectrogram depicting the soundscape at the CC-1/Mary Cove recording site with overlaid detection windows of vessel noise. In the depicted timeframe, all detections formed extended windows of vessel presence. In this case, the vessel noise pattern was indicative of isolated vessel transits. However, the detector performed equally well on irregular, fragmented, or overlapping vessel noise conditions.

### 3.2. Excess noise accuracy

Table 3 summarizes the expected random error to  $\Delta\text{dB}(f)$  for  $f = 80 - 1000$  Hz from estimating underlying natural ambient sound levels by interpolation. Across sites,  $t_{ave}$  ranged between 41 min and 119 min. Assessed for each site individually, a single gap of length  $t_{ave}$  was associated with  $\sigma[\Delta\text{dB}(f)_k]$  from 1.0 to 1.6 dB (see Table 3). The seasonal and diurnal time periods analyzed in this study contained a large number of  $t_{ave}$ -sized gaps, and as a result the random error for these periods were much smaller with an estimated error for  $\Delta\text{dB}$  of 0.02–0.05 dB and 0.03–0.07 dB across sites for seasonal and diurnal categories, respectively.

### 3.3. Annual vessel noise

Average annual vessel noise presence was lowest at NC-1/Otter Channel (24 %), and highest at SS-1/Monarch Head (85 %), reflecting the degree of remoteness and the proximity to urban centers for these sites. The two locations at Northern Vancouver Island (NI-1/2) experienced vessel noise around 50–60 % of the time, and CC-1/Mary Cove, located further north, contained 33 % vessel noise (see Table 4). Vessel activity elevated sound levels at all sites, creating regional annual average excess noise ranging from +1.17 dB (NC-1) to +6.79 dB (SS-1) measured at 80–1000 Hz. Sites with higher average vessel activity also had longer individual time windows of continuous vessel noise presence (40 min for NC-1 compared to 2 h for SS-1) and shorter continuous windows of quiet time (23 min for SS-1 compared to 130 min for NC-1). As a result, the likelihood of individual quiet time windows exceeding 60 min was lower for sites with more vessel activity (41.7 % for SS-1 compared to 91.4 % for NC-1).

Generally, average daily vessel excess noise correlated with the fraction of time vessels were detected (Fig. 8). In contrast, recorded sound levels alone did not provide a meaningful indicator for the level of vessel noise as seasonal and diurnal environmental patterns often outweighed anthropogenic contributions. This effect was amplified as all study sites deployed hydrophones in near-shore, shallow water locations which were in particular impacted by local tides and winds. In fact, no clear correlation was found between detected vessel noise presence and average recorded daily sound levels for any site (Fig. 8). Some sites appear to display an inverse effect (higher recorded sound levels at days with lower vessel presence), potentially because of reduced vessel traffic during poor weather conditions.

### 3.4. Vessel noise impact across the frequency spectrum

Observed excess noise levels varied across the frequency spectrum at all sites. Fig. 9 shows the average annual excess noise caused by vessels

<sup>11</sup> [https://media.fisheries.noaa.gov/dam/migration/characterize\\_sound\\_propagation\\_modeling\\_guidance\\_memo.pdf](https://media.fisheries.noaa.gov/dam/migration/characterize_sound_propagation_modeling_guidance_memo.pdf)

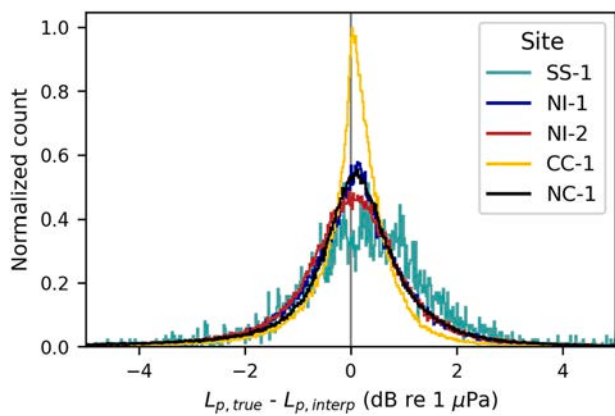


**Fig. 5.** Expected error on natural ambient sound levels during time windows of vessel presence. The curves show the difference between true and estimated sound levels from interpolating vessel noise gaps in the natural ambient time sequence. The interpolation window applied for each site was set to match the average duration of consecutive vessel noise detections, which was 120 min for SS-1 and 60 min for all other sites. (For interpretation of the references to colour in this figure legend, the reader is referred to the web version of this article.)

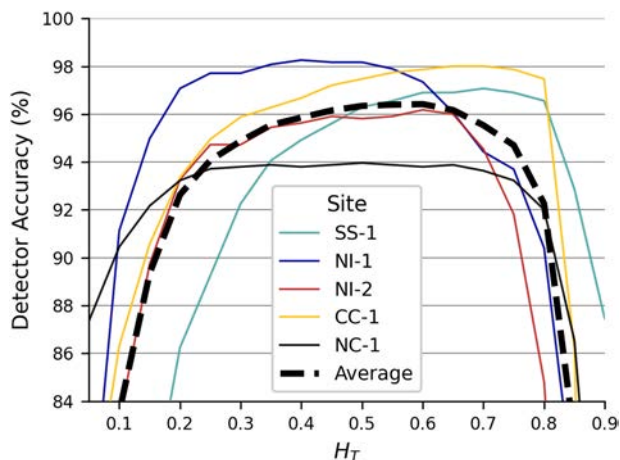


**Fig. 6.** Assessed vessel noise detector accuracy as a function of spectral entropy threshold  $H_T$ . (For interpretation of the references to colour in this figure legend, the reader is referred to the web version of this article.)

for 31 decade frequency bands centered at 20 Hz to 20 kHz for each study site. For most sites, the highest excess noise levels were observed between 200 Hz and 1000 Hz, with the exception of SS-1/Monarch Head, for which excess noise peaked at the 80 Hz decade band. Because all hydrophones were deployed at similar depths, this could reflect a vessel fleet composed to a higher degree of large commercial vessels with average URN at lower frequencies. Across sites, the on average highest excess noise was observed in the 500 Hz decade band. While the majority of excess noise was concentrated at frequencies below 1 kHz, vessels significantly elevated natural soundscape levels at all frequencies within the 27 kHz sensor limit. For example, the 20 kHz decade band showed 33.3 % of the annual average excess noise as compared to the 500 Hz decade band. All sites showed low excess noise at frequencies below 80 Hz in comparison to higher frequencies (e.g., the 20 Hz decade band had 61 % less excess noise with respect to 500 Hz), which likely was an attenuation effect

introduced by the position of hydrophones at less than 40 m below the surface.

### 3.5. Seasonal and diurnal trends

Figs. 10 to 14 show seasonal and diurnal patterns of vessel noise presence and associated excess noise levels for each site and Fig. 15 & 16 compare sites directly. Within these two temporal categories (i.e. month-of-year and hour-of-day),  $\Delta$ dB was expressed as the logarithmic average of all available time segments. All temporal categories except three had at least 75 % of potential data available. The exceptions were November for CC-1 and January/December for NI-1, caused by intermittent recording blackouts (see Fig. S-1 in Supplemental Materials).

Each site showed seasonal and diurnal trends, with commonalities and variations across sites. More vessel noise was present in the months between May and October for all sites, although the month with the most vessel noise varied across sites (May for SS-1, June for CC-1, July for NC-1, August for NI-1/2). This meant that relative impact severity among sites sometimes changed from one month to the other within a calendar year (Fig. 15). For example, across all sites NI-1 experienced the highest vessel excess noise for August, while SS-1 had the highest annual average excess noise. Generally, trends in diurnal and seasonal vessel noise presence matched those for excess noise levels for each site. CC-1 was an exception. Here, vessel noise presence was most prevalent between March and November, while excess noise was slightly stronger from February to June.

Diurnal vessel noise patterns and resulting excess noise levels were generally higher during daylight hours (between 7 am and 5 pm throughout the year), but activity peaked at different times for different sites. For diurnal activity there were notable differences in pattern between vessel presence and excess noise that likely relates to a combination of varying activity among vessel types and in the utilization of traffic lanes. Notably, SS-1 and CC-1 displayed pronounced peaks in excess noise during distinct night time hours potentially associated with peaks in site-specific commercial vessel activity. The patterns described above seen for the 80–1000 Hz band were generally reproduced for a range of octave frequency bands between 31.5 Hz to 16 kHz, and broader decade bands below 27 kHz (see Tables A.5 to A.9 in the Appendix).

### 3.6. Seasonal-diurnal listening space reduction for killer whales

Vessels caused seasonal-diurnal acoustic habitat loss for killer whales at all sites (Fig. 17). The results are expressed as LSR within the 0.5–15 kHz communication band as compared to natural ambient conditions. For visual clarity, the maps were first smoothed with a Gaussian kernel of  $12 \times 2$  pixels (equivalent to 2 h across 12 calendar days, or 24 h-bins total). Results were then binned in steps of 10 % LSR.

The acoustic habitat for killer whales was reduced more during daylight hours and from May to October at all sites except CC-1/Mary Cove. However, the scale of habitat loss differed substantially across the five regional soundscapes. SS-1/Monarch Head experienced LSR of 40 % or higher year-round, with peak-values in August reaching 90 %. NI-1/Flower Island showed similar peak habitat loss (also in August), but LSR during the winter, spring, fall, and during nighttime dropped below 30 %. The soundscape at NC-1/Otter Channel was pristine during the majority of the year with below 10 % LSR at all times except during daylight hours between June and September where maximum acoustic habitat loss of 30 % was observed. The soundscape at CC-1/Mary Cove did not follow a clear seasonal-diurnal pattern, and consistently experienced LSR between 10 and 30 % throughout the year. However, the most severe listening space reduction at this site was also observed mostly during daylight hours.

**Table 2**  
Vessel noise detector performance using  $H_T=0.6$ .

Site ID	Samples	$Pr_{tot}$	$Re_{tot}$	$Pr_{amb}$	$Re_{amb}$	Acc
SS-1	1226	0.992	0.973	0.825	0.943	0.969
NI-1	1261	0.963	0.990	0.987	0.953	0.974
NI-2	1264	0.964	0.964	0.960	0.960	0.962
CC-1	806	0.985	0.956	0.976	0.992	0.979
NC-1	1297	0.957	0.725	0.935	0.992	0.938
Total	5854	0.973	0.916	0.934	0.969	0.964

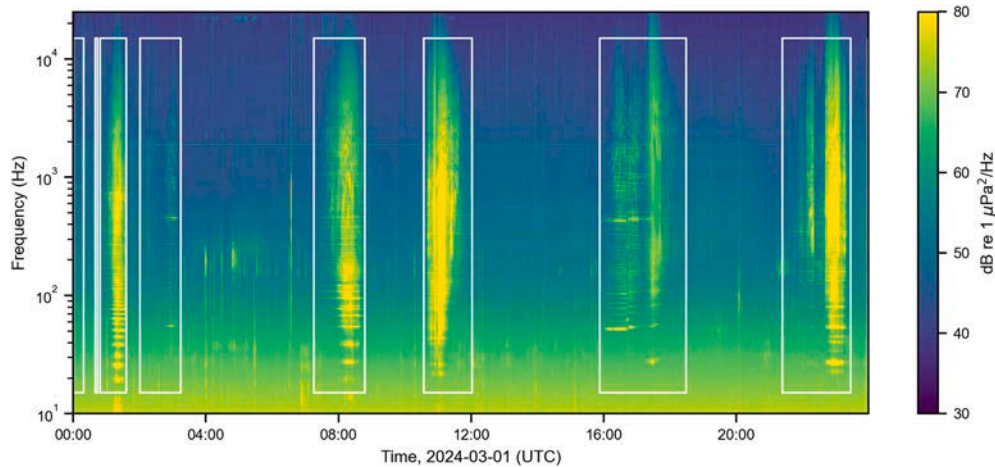


**Fig. 7.** Typical 24 h spectrogram from a study site (CC-1/Mary Cove) showing multiple vessel passages. Signal attenuation below approximately 100 Hz is evident. Received vessel noise levels are highest between 200 and 800 Hz. Boxes indicate vessel noise detections. (For interpretation of the references to colour in this figure legend, the reader is referred to the web version of this article.)

**Table 3**  
Expected random error on monthly (seasonal) and hour-of-day (diurnal) vessel excess noise levels for the 80–1000 Hz frequency band.

Site ID	n	$t_{ave}$ (min)	$\sigma[\Delta dB_k]$	f	$\sigma[\Delta dB_{seasonal}]$	$\sigma[\Delta dB_{diurnal}]$
SS-1	4410	119	1.1	0.85	0.05	0.07
NI-1	71,075	44	1.2	0.58	0.03	0.04
NI-2	111,065	52	1.3	0.53	0.03	0.04
CC-1	183,340	43	1.0	0.33	0.02	0.02
NC-1	284,483	41	1.6	0.24	0.02	0.03

**Table 4**  
Annual average presence of vessel noise, quiet time, vessel excess noise levels ( $\Delta dB$ ; 80–1000 Hz), as well as the average duration of vessel passage ( $W_{tot}$ ) and quiet time windows ( $W_{amb}$ ).

Site ID	Vessel presence	Quiet time	$\Delta dB (dB)$	$W_{tot}$ (min)	$W_{amb}$ (min)	$W_{amb} > 60min$
SS-1	84.9 %	15.1 %	+6.79	118.7	22.4	41.7 %
NI-1	58.0 %	42.0 %	+4.52	43.7	35.6	57.2 %
NI-2	52.7 %	47.3 %	+1.71	52.1	51.4	72.1 %
CC-1	32.7 %	67.3 %	+1.84	42.8	82.3	82.5 %
NC-1	23.6 %	76.4 %	+1.17	40.9	130.0	91.4 %

## 4. Discussion

### 4.1. Adapting the framework to new data sets and use cases

The vessel detection framework was robust within a variety of soundscapes and vessel activities. We speculate that the entropy threshold used in the detector is universal, therefore potentially eliminating the need for either data annotation or detector parametrization when applied to new datasets. While it was possible to optimize detector performance by applying a site-specific threshold, the improvement was marginal, with an average accuracy of 96.6 % across sites, as compared to 96.4 % using a single threshold for the five sites analyzed in this study.

A vessel noise framework without the need for annotating acoustic recordings, or conducting other custom parametrization provides a computationally efficient, analytical, and replicable tool for assessing the impact of vessel noise on marine soundscapes. In this study, 300 s of consecutive vessel noise presence were required to trigger the detector, which would impose some restrictions on a duty-cycled recording setup. However, the detector accuracy was similar when applied to isolated 60-second segments. Therefore, it is possible to apply the detection framework with slight modifications to any acoustic data set that constitutes data segments of at least 60 s in duration that are sampled at a rate of 2 kHz or higher. Due to the computational efficiency, the detector could also be deployed for near real-time systems, such as inside coastal buoys, on ultra low-power computing modules.

### 4.2. Limitations

Shallow-water hydrophone installations limit the ability to analyze the lowest vessel noise frequencies (< 50 Hz). Selective frequency attenuation can also depend on the position of the source in the water column and its distance to the receiver, as well as on local bathymetry. As a result, the exact signal attenuation at low frequencies is dynamic and site-dependent. However, installations in deeper water are often expensive and shallow-water deployments may present the most effective means of generating the quantity and spatial distribution of acoustic data required to understand the broad impact of vessel noise for coastal ecosystems. The framework introduced in this study uses ecosystem-based metrics, where acoustic monitoring sites may act as proxies for larger regions. In this context, the placement of hydrophone stations requires consideration to ensure results are representative for a regional ecosystem. For example, the two datasets recorded in the same broader region (NI-1, NI-2) were located within a few kilometres of each other and similar vessel presence was detected throughout the year. However, vessel excess noise was substantially higher at NI-1 than at NI-2. While

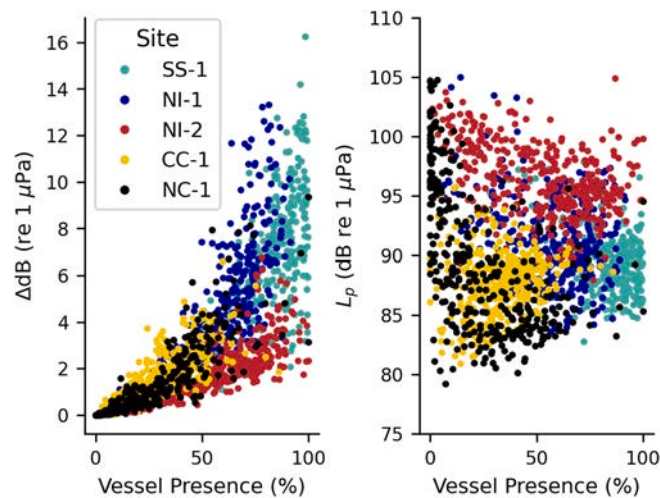


**Fig. 8.** Relationship of daily average vessel noise presence with vessel excess noise  $\Delta$ dB (left) and 80–1000 Hz sound levels  $L_p$  (right) for each site for days with more than 50 % recording effort. A positive relationship between vessel presence and  $\Delta$ dB is seen, while no such relationship is evident between vessel presence and sound levels. (For interpretation of the references to colour in this figure legend, the reader is referred to the web version of this article.)

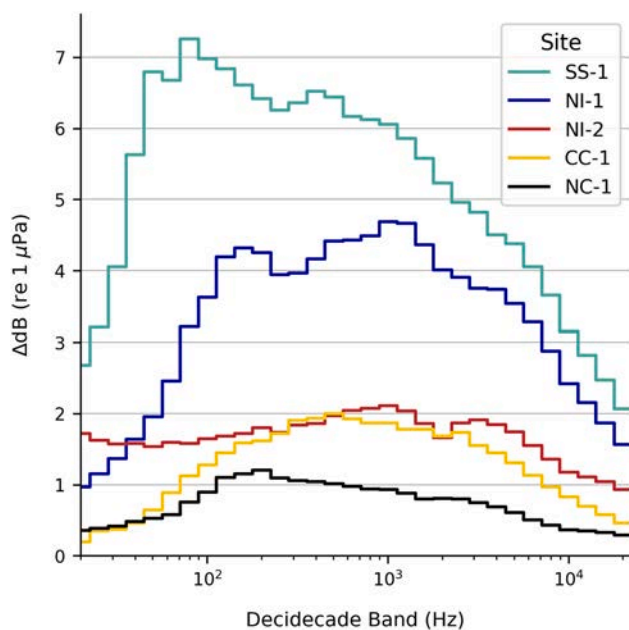


**Fig. 9.** Average annual vessel excess noise levels for 31 decidecade frequency bands between 20 Hz and 20 kHz) for all five sites.

some of this discrepancy may be attributed to different vessel types and shipping lanes, average monthly recorded sound levels were higher at NI-2 across the frequency spectrum and as a result, the impact of vessels on the soundscape was lower. NI-2 was deployed in an area with particularly strong tidal currents, and we suspect that these local conditions affected the observed vessel noise impact. Only if these particular conditions are representative for the ecosystem in which the hydrophone was deployed in, results with respect to vessel noise impact are meaningful. Finally, using observational data, the accuracy of results is tied to the performance of the recording instrument. For example, the month-to-month vessel noise presence at CC-1 did not always align with corresponding excess noise levels. It is possible that this reflects real seasonal differences in vessel types and traffic lanes (i.e., how much excess noise a typical vessel produces). But because overall variations at this site were small (below 1 dB month-to-month), it cannot be ruled out that the hydrophone experienced a shift in self-noise, introducing a

subtle systematic error.

#### 4.3. Implications for underwater noise monitoring and management

This study presents a new and accessible approach to quantify vessel noise at multiple temporal scales relevant for management using hydrophone data. The levels of vessel noise are reported as excess noise and account for noise contributed by vessels above natural ambient noise levels. Underwater noise management efforts to date have been limited by the inability to reliably capture total vessel noise contributions in soundscapes and quantify the less tractable component sources of vessel noise from non-AIS vessels. The ability to fully quantify the contribution of vessel noise enables a more accurate computation of LSR and quiet time (i.e. the absence of vessel noise), for assessing acoustic habitat quality. Underwater noise management efforts encompass approaches to limit anthropogenic noise exposure on marine fauna and their habitats both spatially and temporally. The framework can be applied to assess efforts to reduce noise from marine vessels by monitoring vessel noise contributions at representative sites over multiple temporal scales. While the quantification of vessel noise contributions are site specific, they can be indicative of sub-regional conditions depending on hydrophone location and local natural ambient noise conditions. The explicit quantification of vessel noise levels can be used to set regional noise reduction targets and limits for vessel noise contributions to the natural soundscape at multiple temporal scales. As demonstrated in this study, the excess vessel noise component varies greatly from region to region within BC. The Salish Sea site (SS-1) is reflective of a degraded natural soundscape with large additions of vessel noise and sparse windows of quiet time. Restoring this soundscape for marine mammals could be achieved by setting a regional reduction target for vessel noise in excess of natural ambient levels. In contrast, the Central and North Coast sites (CC-1, NC-1) are indicative of relatively pristine soundscapes. Managing underwater noise for such conditions could encompass setting thresholds for vessel excess noise levels. Similar management objectives could be designed around LSR levels or quiet time for maintaining pristine or improving degraded soundscape conditions.

#### 5. Summary

This study presents a framework for the acoustic detection and quantification of vessel noise in marine soundscapes. The detector captures noise from commercial vessels, as well as those not equipped

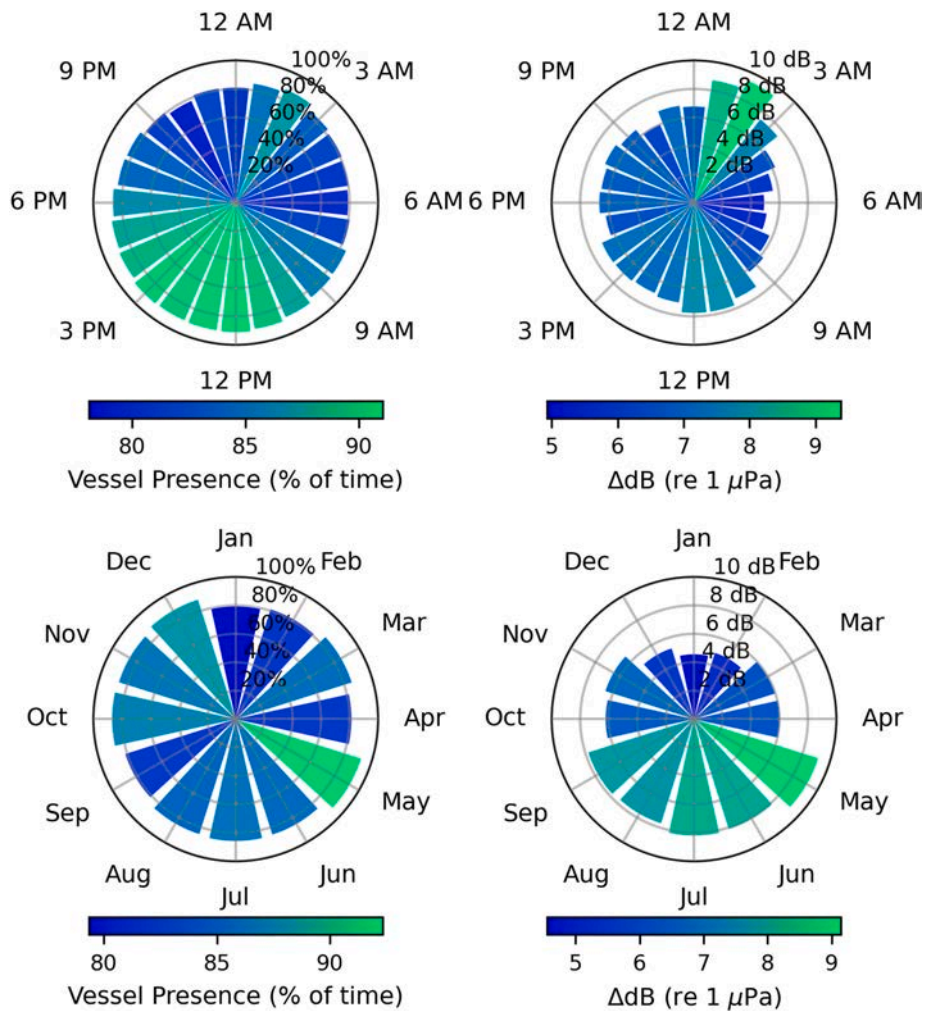


**Fig. 10.** Annual vessel noise presence (left) and vessel excess noise (right) for each calendar month (top) and local hour-of-day (bottom) observed at the SS-1/ Monarch Head site. The coloration of wedges reflects the range of values within each plot: from lowest (blue) to highest (green). Excess noise is shown for the 80–1000 Hz frequency band. (For interpretation of the references to colour in this figure legend, the reader is referred to the web version of this article.)

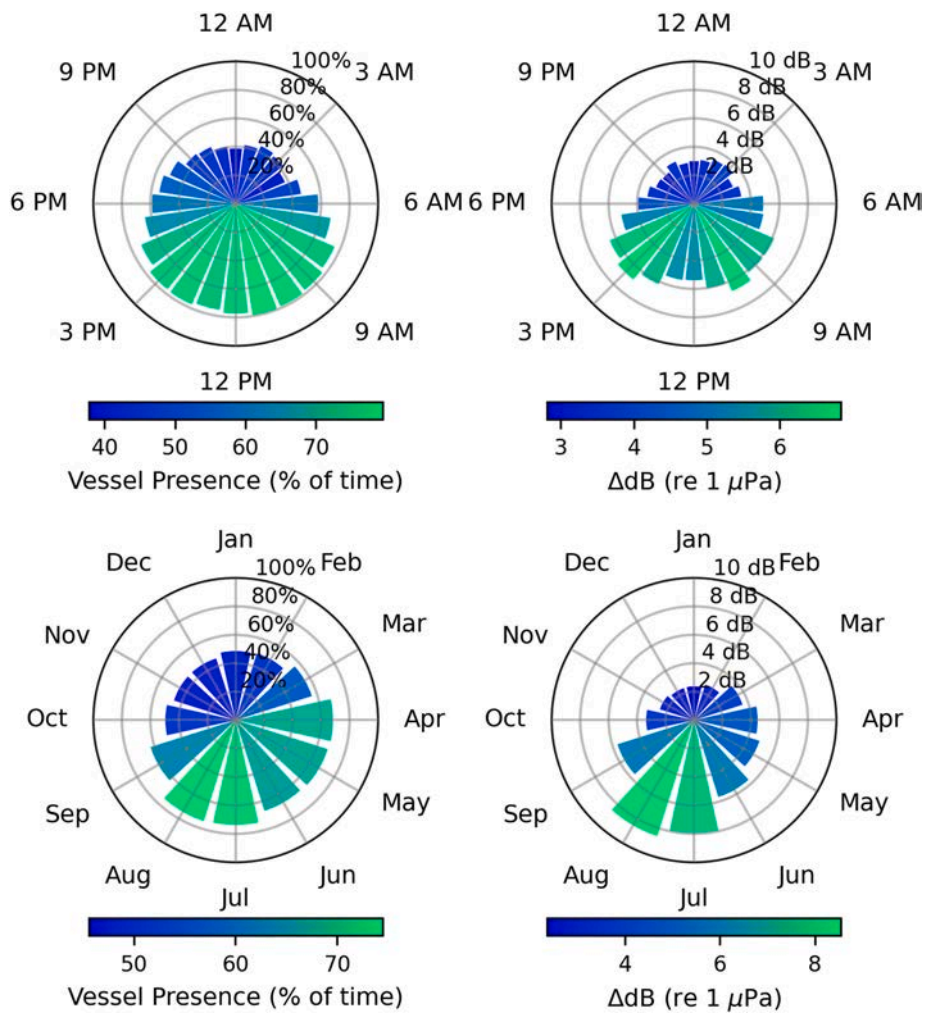


**Fig. 11.** Annual vessel noise presence (left) and vessel excess noise (right) for each calendar month (top) and local hour-of-day (bottom) observed at the NI-1/Flower Island site. The coloration of wedges reflects the range of values within each plot: from lowest (blue) to highest (green). Excess noise is shown for the 80–1000 Hz frequency band. (For interpretation of the references to colour in this figure legend, the reader is referred to the web version of this article.)

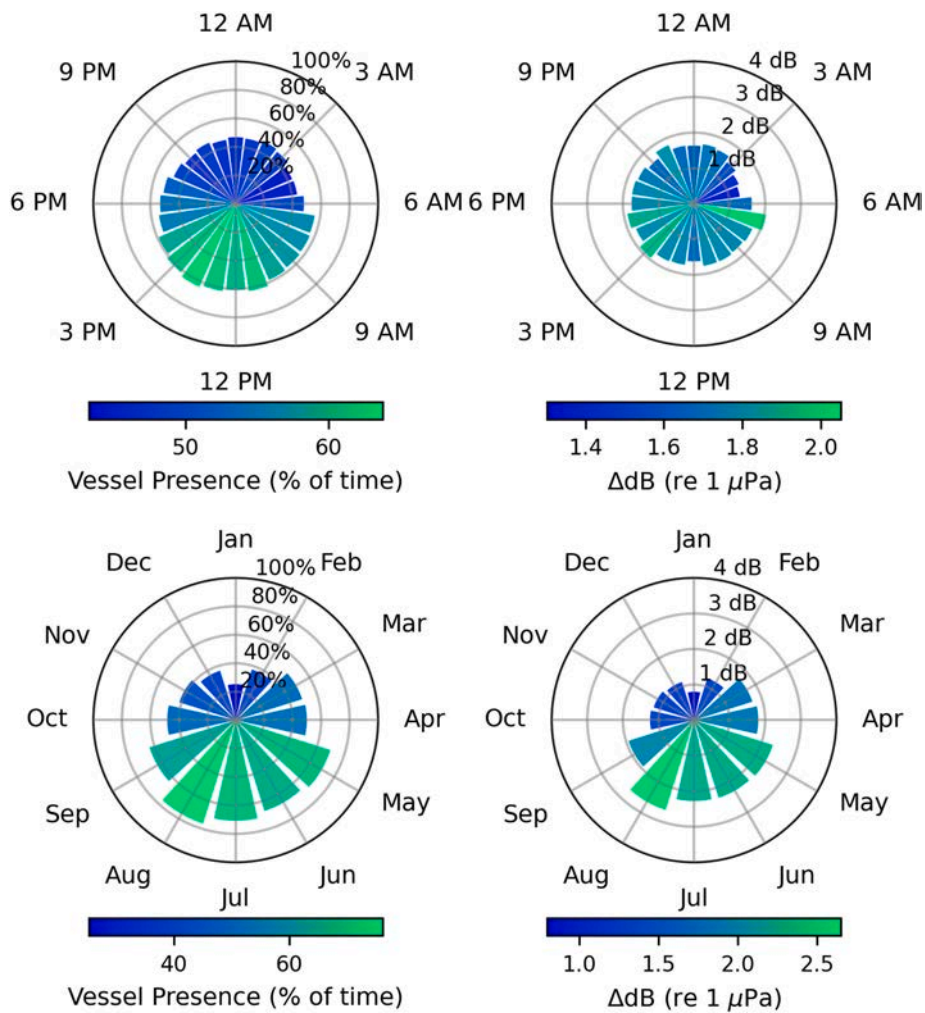


**Fig. 12.** Annual vessel noise presence (left) and vessel excess noise (right) for each calendar month (top) and local hour-of-day (bottom) observed at the NI-2/ Cracroft Point site. The coloration of wedges reflects the range of values within each plot: from lowest (blue) to highest (green). Excess noise is shown for the 80–1000 Hz frequency band. (For interpretation of the references to colour in this figure legend, the reader is referred to the web version of this article.)

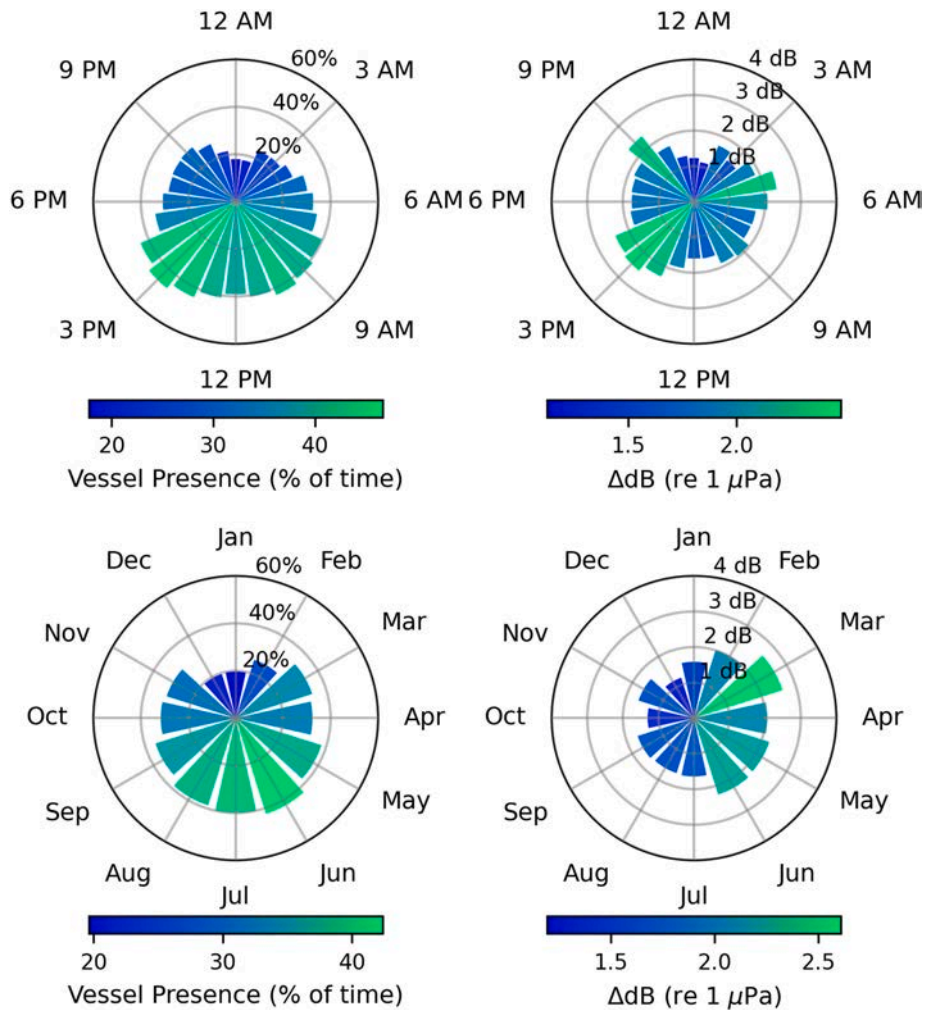


**Fig. 13.** Annual vessel noise presence (left) and vessel excess noise (right) for each calendar month (top) and local hour-of-day (bottom) observed at the CC-1/Mary Cove site. The coloration of wedges reflects the range of values within each plot: from lowest (blue) to highest (green). Excess noise is shown for the 80–1000 Hz frequency band. (For interpretation of the references to colour in this figure legend, the reader is referred to the web version of this article.)

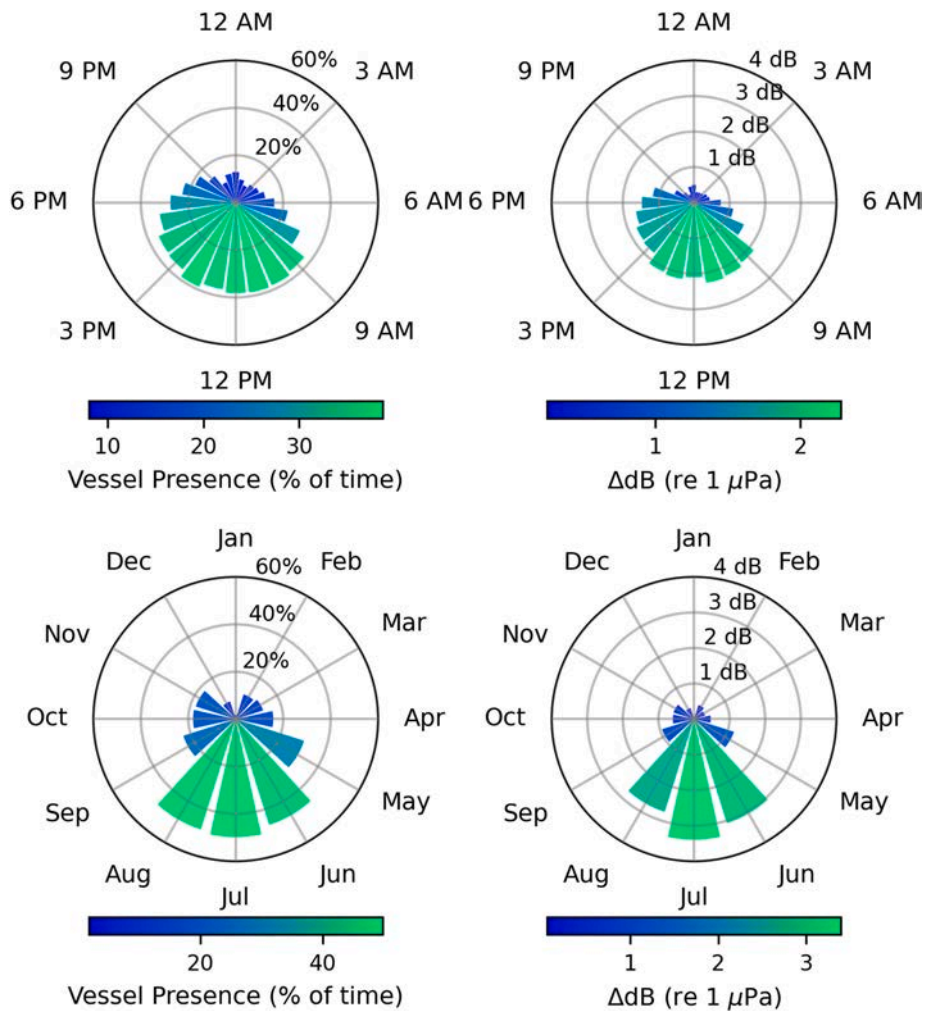


**Fig. 14.** Annual vessel noise presence (left) and vessel excess noise (right) for each calendar month (top) and local hour-of-day (bottom) observed at the NC-1/Otter Channel site. The coloration of wedges reflects the range of values within each plot: from lowest (blue) to highest (green). Excess noise is shown for the 80–1000 Hz frequency band. (For interpretation of the references to colour in this figure legend, the reader is referred to the web version of this article.)

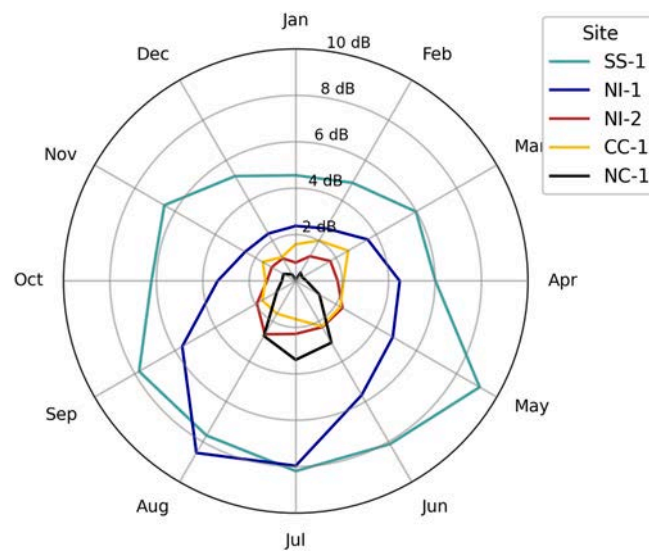


**Fig. 15.** Annual excess noise across calendar months for all five study sites in direct comparison measured for the 80–1000 Hz frequency band: SS-1 (green), NI-1 (blue), NI-2 (red), CC-1 (yellow), NC-1 (black). (For interpretation of the references to colour in this figure legend, the reader is referred to the web version of this article.)

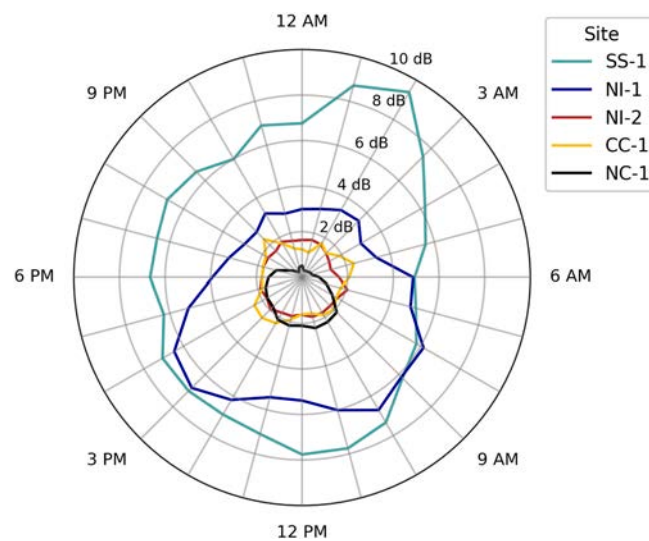


**Fig. 16.** Annual excess noise across hours-of-day for all five study sites in direct comparison measured for the 80–1000 Hz frequency band: SS-1 (green), NI-1 (blue), NI-2 (red), CC-1 (yellow), NC-1 (black). (For interpretation of the references to colour in this figure legend, the reader is referred to the web version of this article.)

with AIS, allowing quantification of total vessel noise impact on regional aquatic ecosystems, thus filling a current knowledge gap for marine management. The framework uses an analytical approach that performed robustly on long-term, real-world data and a range of soundscapes. Applied to a full year of acoustic data from five recording sites across the coast of Western Canada, the detector provided an average accuracy of 96.4 % across all sites, vessel types, and environmental conditions. Annual average listening space reduction for killer whales caused by vessel noise ranged from 6.6 % to 46.9 % across sites and seasonally reached values above 80 % in two of the five study areas. These baselines will help to monitor trends in underwater noise in the context of changing vessel activity and mitigation policies. The substantial variation of noise impact observed between sites highlights the necessity to assess the impact of underwater vessel noise within a regional or local context. With an increasing number of operational

underwater listening stations worldwide, there is a growing opportunity for spatial and temporal mapping of vessel noise. With minimal required customization, the vessel noise detection framework presented here provides a reliable, transferrable, and cost-effective tool for better understanding the relationship between prevalent vessel noise levels in marine soundscapes and their impact on regional ecosystems.

**CRedit authorship contribution statement**

**B. Hendricks:** Writing – original draft, Visualization, Validation, Supervision, Software, Resources, Project administration, Methodology, Investigation, Formal analysis, Data curation, Conceptualization. **M.K. Pine:** Writing – review & editing, Supervision, Project administration, Methodology, Conceptualization. **G. Baer:** Writing – review & editing, Validation, Project administration, Data curation. **M. Welton:** Writing –

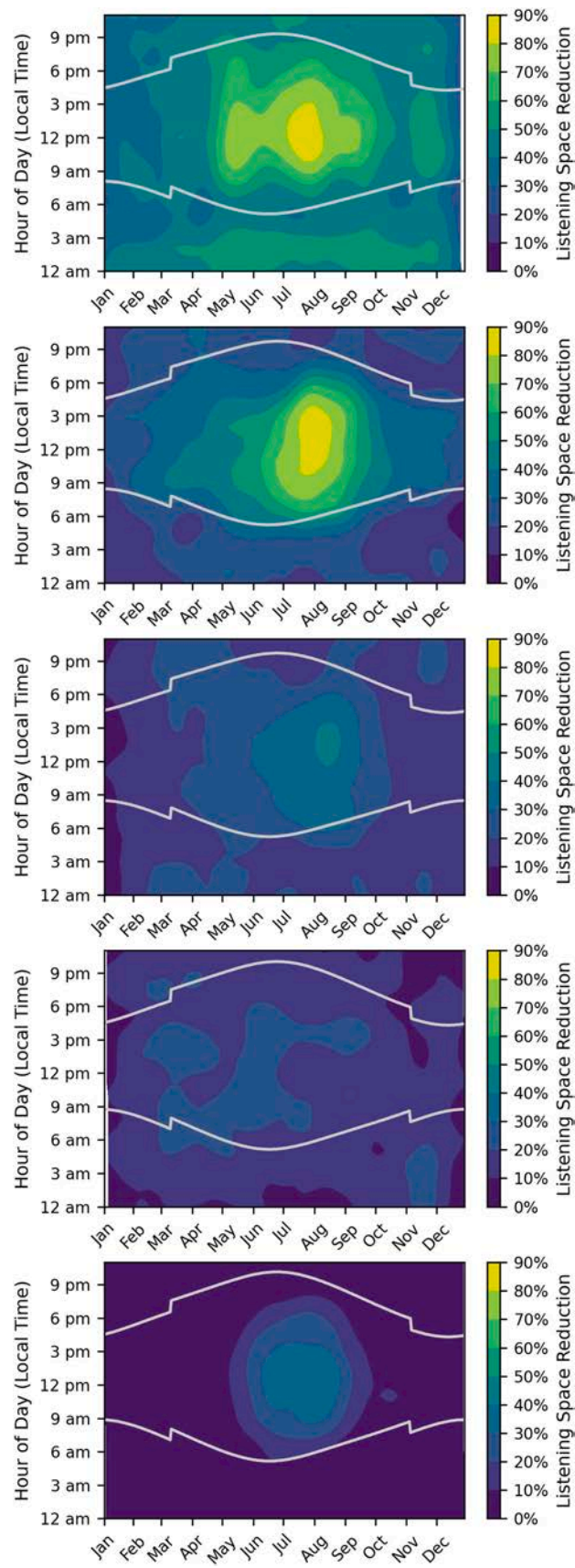


**Fig. 17.** Seasonal-diurnal listening space reduction for the 0.5–15 kHz killer whale communication band. Sunrise/sunset times are shown as overlays. The original data array was smoothed and subsequently binned (see the text for details). From top to bottom: SS-1/Monarch Head, NI-1/Flower Island, NI-2/Cracroft Point, CC-1/Mary Cove, NC-1/Otter Channel.

review & editing, Resources, Data curation. **H.K. Symonds:** Writing – review & editing, Project administration, Data curation. **D.T. Dakin:** Writing - review & editing, Conceptualization. **H.M. Alidina:** Writing – review & editing, Project administration, Funding acquisition. **C.R. Picard:** Writing – review & editing, Resources, Project administration. **J. Wray:** Writing – review & editing, Supervision, Resources, Project administration, Funding acquisition, Data curation, Conceptualization.

**Declaration of competing interest**

The authors declare that they have no known competing financial interests or personal relationships that could have appeared to influence the work reported in this paper.

**Acknowledgments**

The North Coast Cetacean Society acknowledges financial support

from the Environmental Foundation Greenpeace, Fisheries and Oceans Canada - Canada Nature Fund for Aquatic Species at Risk, the Save our Seas Foundation, the MakeWay Foundation, the Donner Canadian Foundation, and the Willow Grove Foundation. WWF-Canada support for this work was made possible with funds for the SWAG Project (Ships Whales & Acoustics in Gitga’at Territory) received from Fisheries & Oceans Canada (18-23-25-PA-MEQ-042) and the Audain Foundation. The use of acoustic data for this project was gratefully granted individually by the Kitsoo Xai’xais Nation, the SWAG Project, the Pacific Orca Society/OrcaLab, and SIMRES (Saturna Island Marine Research and Education Society). We would also like to thank Oliver Kirsebom and Dom Tollit for feedback and advice on study design and for feedback on the manuscript, as well as Joel Mellish and Jeff Bosma along with many others for realizing community-based acoustic monitoring solutions in BC waters.

**Appendix A. Monthly vessel excess noise levels**

**Table A.5**  
Seasonal vessel excess noise levels (ΔdB) for octave and decade bands; SS-1/Monarch Head.

Month	Octave Bands (Hz)										Decade Bands (Hz)		
	31.5	63	125	250	500	1000	2000	4000	8000	16,000	10–100	100–1000	1000–10,000
Jan	4.16	6.03	4.98	4.08	3.76	3.50	3.19	2.74	2.16	1.65	4.62	4.28	2.93
Feb	4.28	6.24	5.38	4.35	4.30	3.94	3.50	3.08	2.50	1.96	4.80	4.69	3.28
Mar	5.07	7.30	6.49	5.40	5.25	4.84	4.32	3.86	3.23	2.23	5.75	5.75	4.09
Apr	4.87	6.85	6.25	5.38	5.33	4.99	4.50	3.82	3.13	2.11	5.23	5.70	4.06
May	5.69	8.66	8.94	8.63	8.64	7.85	7.18	6.42	4.80	2.92	6.60	8.89	6.62
Jun	5.11	7.80	8.02	7.58	7.65	6.66	5.39	4.77	3.66	2.30	5.94	7.90	5.05
Jul	4.19	7.08	7.95	7.86	7.80	7.21	6.24	5.46	4.19	2.54	5.16	8.11	5.74
Aug	4.35	7.02	7.51	7.11	7.28	7.08	5.69	5.13	4.15	2.60	5.19	7.54	5.41
Sep	4.75	7.61	7.68	7.13	7.27	6.89	5.53	4.62	3.74	2.36	5.52	7.58	5.06
Oct	4.14	6.52	6.33	5.65	5.70	5.54	4.69	4.05	3.26	2.15	4.85	6.00	4.32
Nov	4.57	7.10	6.70	5.97	6.37	6.36	5.33	4.75	3.78	2.57	5.24	6.45	5.00
Dec	4.32	6.48	5.66	4.56	4.48	4.43	4.08	3.39	2.73	2.16	4.96	4.90	3.68

**Table A.6**  
Seasonal vessel excess noise levels (ΔdB) for octave and decade bands; NI-1/Flower Island.

Month	Octave Bands (Hz)										Decade Bands (Hz)		
	31.5	63	125	250	500	1000	2000	4000	8000	16,000	10–100	100–1000	1000–10,000
Jan	0.87	1.56	2.27	2.16	2.33	2.67	2.39	2.02	1.58	1.02	1.23	2.39	2.20
Feb	1.00	1.83	2.59	2.45	2.58	2.84	2.59	2.28	1.83	1.27	1.41	2.60	2.49
Mar	1.15	2.11	3.25	3.25	3.64	4.03	3.65	3.14	2.44	1.49	1.58	3.59	3.41
Apr	1.49	2.64	3.90	4.41	4.75	4.87	4.27	3.74	2.88	1.81	2.02	4.49	3.98
May	1.72	2.83	4.17	4.74	5.55	5.47	4.75	4.14	3.14	2.04	2.26	4.96	4.40
Jun	1.96	3.37	4.97	5.33	6.37	6.13	5.39	4.66	3.51	2.33	2.56	5.76	4.95
Jul	3.10	5.68	7.68	7.16	7.00	7.06	6.38	5.85	4.56	3.31	4.21	7.86	6.02
Aug	3.30	5.84	8.49	7.95	7.60	7.93	6.83	6.04	4.67	3.22	4.35	8.65	6.30
Sep	2.02	3.43	5.15	5.58	5.57	5.54	4.43	4.29	3.48	2.45	2.56	5.73	4.36
Oct	1.14	2.09	3.08	3.21	3.38	3.57	3.07	2.82	2.33	1.60	1.53	3.36	2.95
Nov	0.88	1.71	2.28	2.32	2.49	3.10	2.86	2.56	2.01	1.23	1.25	2.55	2.72
Dec	0.79	1.44	2.13	2.08	2.34	2.98	2.73	2.41	1.94	1.27	1.09	2.42	2.60

**Table A.7**  
Seasonal vessel excess noise levels ( $\Delta$ dB) for octave and decade bands; NI-2/Cracroft Point.

Month	Octave Bands (Hz)										Decade Bands (Hz)		
	31.5	63	125	250	500	1000	2000	4000	8000	16,000	10–100	100–1000	1000–10,000
Jan	0.50	0.56	0.71	0.73	0.81	1.07	1.12	1.20	0.90	0.57	0.51	0.81	1.12
Feb	0.80	0.94	1.06	1.13	1.36	1.45	1.45	1.57	1.10	0.71	0.86	1.26	1.44
Mar	1.47	1.31	1.35	1.68	2.02	2.01	1.85	2.00	1.48	0.96	1.63	1.75	1.84
Apr	1.31	1.26	1.49	1.82	2.23	2.13	1.76	1.91	1.41	1.01	1.49	1.89	1.77
May	2.30	2.19	2.15	2.43	2.71	2.48	1.87	1.79	1.43	1.21	2.74	2.40	1.77
Jun	2.06	2.00	2.04	2.33	2.76	2.53	1.77	1.68	1.34	1.09	2.18	2.35	1.66
Jul	2.19	2.09	2.10	2.33	2.59	2.57	1.89	1.83	1.41	1.26	2.29	2.34	1.77
Aug	2.52	2.45	2.70	2.84	2.61	3.00	2.45	2.42	1.75	1.44	2.87	2.72	2.28
Sep	1.78	1.89	2.19	1.95	1.81	2.14	1.94	1.99	1.55	1.33	1.82	1.93	1.87
Oct	1.32	1.35	1.39	1.21	1.18	1.35	1.31	1.48	1.14	0.90	1.33	1.22	1.33
Nov	1.14	1.12	1.23	1.07	1.14	1.56	1.63	1.69	1.20	0.87	1.20	1.19	1.56
Dec	0.87	0.91	1.03	0.97	1.19	1.54	1.55	1.61	1.12	0.80	0.91	1.14	1.50

**Table A.8**  
Seasonal vessel excess noise levels ( $\Delta$ dB) for octave and decade bands; CC-1/Mary Cove.

Month	Octave Bands (Hz)										Decade Bands (Hz)		
	31.5	63	125	250	500	1000	2000	4000	8000	16,000	10–100	100–1000	1000–10,000
Jan	0.36	0.79	1.19	1.47	1.71	1.68	1.74	1.56	1.10	0.61	0.52	1.62	1.58
Feb	0.48	1.03	1.52	1.87	2.18	2.13	2.13	1.80	1.24	0.64	0.67	2.05	1.87
Mar	0.55	1.27	1.92	2.30	2.75	2.70	2.72	2.37	1.66	0.84	0.80	2.58	2.43
Apr	0.55	1.18	1.81	2.12	2.22	2.07	2.02	1.75	1.22	0.71	0.77	2.17	1.78
May	0.44	1.02	1.83	2.35	2.45	2.19	1.93	1.51	0.92	0.49	0.66	2.31	1.62
Jun	0.43	1.19	1.99	2.31	2.36	1.95	1.65	1.24	0.78	0.50	0.75	2.26	1.37
Jul	0.55	0.97	1.43	1.69	1.74	1.53	1.31	1.00	0.64	0.44	0.74	1.66	1.10
Aug	0.46	0.96	1.47	1.67	1.73	1.50	1.22	0.85	0.52	0.42	0.68	1.66	0.97
Sep	0.40	0.98	1.44	1.68	1.76	1.54	1.30	0.93	0.62	0.48	0.66	1.66	1.05
Oct	0.25	0.63	1.09	1.30	1.48	1.48	1.46	1.20	0.83	0.57	0.42	1.35	1.26
Nov	0.27	0.67	1.15	1.34	2.00	2.24	2.20	2.19	1.65	0.98	0.44	1.67	2.07
Dec	0.16	0.46	0.71	0.99	1.44	1.50	1.55	1.36	0.99	0.59	0.31	1.23	1.40

**Table A.9**  
Seasonal vessel excess noise levels ( $\Delta$ dB) for octave and decade bands; NC-1/Otter Channel.

Month	Octave Bands (Hz)										Decade Bands (Hz)		
	31.5	63	125	250	500	1000	2000	4000	8000	16,000	10–100	100–1000	1000–10,000
Jan	0.02	0.02	0.04	0.06	0.06	0.06	0.05	0.04	0.02	0.02	0.02	0.06	0.05
Feb	0.20	0.23	0.35	0.47	0.39	0.36	0.31	0.27	0.15	0.08	0.22	0.42	0.29
Mar	0.17	0.19	0.27	0.37	0.31	0.28	0.29	0.28	0.16	0.08	0.17	0.33	0.26
Apr	0.27	0.31	0.43	0.48	0.46	0.43	0.42	0.36	0.24	0.17	0.27	0.47	0.37
May	0.39	0.53	1.08	1.25	1.16	1.07	0.95	0.77	0.46	0.34	0.54	1.22	0.81
Jun	1.06	1.89	3.10	2.95	2.36	2.09	1.83	1.58	1.06	0.77	1.51	3.00	1.60
Jul	1.17	2.07	3.46	3.30	2.70	2.51	2.23	1.84	1.16	0.93	1.47	3.43	1.88
Aug	1.02	1.64	2.64	2.70	2.40	2.08	1.81	1.52	0.97	0.70	1.26	2.75	1.54
Sep	0.41	0.49	0.81	0.99	0.90	0.74	0.59	0.49	0.32	0.26	0.45	0.95	0.50
Oct	0.37	0.41	0.60	0.62	0.66	0.61	0.52	0.42	0.24	0.15	0.36	0.64	0.44
Nov	0.34	0.37	0.50	0.61	0.62	0.53	0.46	0.34	0.22	0.21	0.38	0.60	0.41
Dec	0.12	0.15	0.24	0.27	0.33	0.32	0.22	0.20	0.15	0.11	0.14	0.33	0.21

**Appendix A. Supplementary data**

Supplementary data to this article can be found online at <https://doi.org/10.1016/j.marpolbul.2025.118150>.

**Data availability**

Data will be made available on request.

**References**

Ainslie, M.A., Halvorsen, M.B., Robinson, S.P., 2022. A terminology standard for underwater acoustics and the benefits of international standardization. *IEEE J. Ocean. Eng.* 47, 179–200. <https://doi.org/10.1109/JOE.2021.3085947>.  
 Alexandri, T., Diamant, R., 2024. Detection and characterization of ship underwater radiated narrowband noise. *Comput. Netw.* 248, 110480. <https://doi.org/10.1016/j.comnet.2024.110480>.

- Arveson, P.T., Vendittis, D.J., 2000. Radiated noise characteristics of a modern cargo ship. *J. Acoust. Soc. Am.* 107, 118–129. <https://doi.org/10.1121/1.428344>.
- Aslam, M.A., Zhang, L., Liu, X., Irfan, M., Xu, Y., Li, N., Zhang, P., Jiangbin, Z., Yaan, L., 2024. Underwater sound classification using learning based methods: a review. *Expert Syst. Appl.* 255, 124498. <https://doi.org/10.1016/j.eswa.2024.124498>.
- Barlett, M.L., Wilson, G.R., 2002. Characteristics of small boat signatures. *J. Acoust. Soc. Am.* 112, 2221. <https://doi.org/10.15760/etd.728>.
- Blair, H.B., Merchant, N.D., Friedlaender, A.S., Wiley, D.N., Parks, S.E., 2016. Evidence for ship noise impacts on humpback whale foraging behaviour. *Biol. Lett.* 12, 20160005. <https://doi.org/10.1098/rsbl.2016.0005>.
- Bougher, B.B., Hood, J., Theriault, J., Moors, H., 2012. Generalized Marine Mammal Detection Based on Improved Band-Limited Processing, in: Proceedings of Meetings on Acoustics, Volume 17. AIP Publishing. <https://doi.org/10.1121/1.4773596>.
- Breeze, H., Nolet, V., Thomson, D., Wright, A.J., Marotte, E., Sanders, M., 2022. Efforts to advance underwater noise management in Canada: introduction to the marine pollution bulletin special issue. *Mar. Pollut. Bull.* 178, 113596. <https://doi.org/10.1016/j.marpolbul.2022.113596>.
- Burnham, R.E., Vagle, S., O'Neill, C., Trounce, K., 2021. The efficacy of management measures to reduce vessel noise in critical habitat of southern resident killer whales in the salish sea. *Front. Mar. Sci.* 8, 664691. <https://doi.org/10.3389/fmars.2021.664691>.
- Burnham, R.E., Vagle, S., Thupaki, P., Thornton, S.J., 2023. Implications of wind and vessel noise on the sound fields experienced by southern resident killer whales orcinus orca in the salish sea. *Endanger. Species Res.* 50, 31–46. <https://doi.org/10.3354/esr01217>.
- Chou, E., Southall, B.L., Robards, M., Rosenbaum, H.C., 2021. International policy, recommendations, actions and mitigation efforts of anthropogenic underwater noise. *Ocean Coast. Manag.* 202, 105427. <https://doi.org/10.1016/j.ocecoaman.2020.105427>.
- Clark, C.W., Ellison, W.T., Southall, B.L., Hatch, L., Van Parijs, S.M., Frankel, A., Ponirakis, D., 2009. Acoustic masking in marine ecosystems: intuitions, analysis, and implication. *Mar. Ecol. Prog. Ser.* 395, 201–222. <https://doi.org/10.3354/meps08402>.
- C. Erbe, Underwater noise of small personal watercraft (jet skis), *J. Acoust. Soc. Am.* 133 (2013) EL326–EL330. doi:<https://doi.org/10.1121/1.4795220>.
- Erbe, C., King, A.R., 2008. Automatic detection of marine mammals using information entropy. *J. Acoust. Soc. Am.* 124, 2833–2840. <https://doi.org/10.1121/1.2982368>.
- C. Erbe, S. Liong, M. W. Koessler, A. J. Duncan, T. Gourlay, Underwater sound of rigid-hulled inflatable boats, *J. Acoust. Soc. Am.* 139 (2016) EL223–EL227. doi:<https://doi.org/10.1121/1.4954411>.
- C. Erbe, A. MacGillivray, R. Williams, Mapping cumulative noise from shipping to inform marine spatial planning, *J. Acoust. Soc. Am.* 132 (2012) EL423–EL428. doi:<https://doi.org/10.1121/1.4758779>.
- Erbe, C., Marley, S.A., Schoeman, R.P., Smith, J.N., Trigg, L.E., Embling, C.B., 2019. The effects of ship noise on marine mammals—a review. *Front. Mar. Sci.* 6, 606. <https://doi.org/10.3389/fmars.2019.00606>.
- Ferguson, E.L., Clayton, H.M., Sakai, T., 2023. Acoustic indices respond to specific marine mammal vocalizations and sources of anthropogenic noise. *Front. Mar. Sci.* 10, 1025464. <https://doi.org/10.3389/fmars.2023.1025464>.
- Gaydos, J.K., Thixton, S., Donatuto, J., 2015. Evaluating threats in multinational marine ecosystems: a coast salish first nations and tribal perspective. *PLoS One* 10, e0144861. <https://doi.org/10.1371/journal.pone.0144861>.
- Gomez, C., Lawson, J., Wright, A.J., Buren, A., Tollit, D., Lesage, V., 2016. A systematic review on the behavioural responses of wild marine mammals to noise: the disparity between science and policy. *Can. J. Zool.* 94, 801–819. <https://doi.org/10.1139/cjz-2016-0098>.
- Heise, K., Barrett-Lennard, L., Chapman, N., Dakin, D., Erbe, C., Hannay, D., Merchant, N., Pilkington, J., Thornton, S., Tollit, D., et al., 2017. Proposed metrics for the management of underwater noise for southern resident killer whales. *Coastal Ocean Report Series* 2, 30. <https://doi.org/10.18258/6457>.
- Heise, K.A., 2008. Recovery strategy for the northern and southern resident killer whales (Orcinus orca) in Canada. Fisheries and Oceans Canada. <https://doi.org/10.53846/goediss-6292>.
- B. Hendricks, E. M. Keen, J. L. Wray, H. M. Alidina, L. McWhinnie, H. Meuter, C. R. Picard, T. A. Gulliver, Automated monitoring and analysis of marine mammal vocalizations in coastal habitats, in: 2018 OCEANS-MTS/IEEE Kobe techno-oceans (OTO), IEEE, 2018, pp. 1–10. doi:<https://doi.org/10.1109/oceanskobe.2018.8559432>.
- Hildebrand, J.A., 2009. Anthropogenic and natural sources of ambient noise in the ocean. *Mar. Ecol. Prog. Ser.* 395, 5–20. <https://doi.org/10.3410/f.2111967.1706066>.
- Holt, M.M., Noren, D.P., Veirs, V., Emmons, C.K., Veirs, S., 2009. Speaking up: killer whales (orcinus orca) increase their call amplitude in response to vessel noise. *J. Acoust. Soc. Am.* 125, EL27–EL32. <https://doi.org/10.1121/1.3040028>.
- IMO, Revised guidelines for the reduction of underwater radiated noise from shipping to address adverse impacts on marine life, 2023. URL: [https://wwwcdn.imo.org/localresources/en/Documents/MEPC.1-Circ.906%20-%20Revised%20Guidelines%20For%20The%20Reduction%20Of%20Underwater%20Radiated%20NoiseFrom%20Shipping%20To%20Address...%20\(Secretariat\).pdf](https://wwwcdn.imo.org/localresources/en/Documents/MEPC.1-Circ.906%20-%20Revised%20Guidelines%20For%20The%20Reduction%20Of%20Underwater%20Radiated%20NoiseFrom%20Shipping%20To%20Address...%20(Secretariat).pdf). doi:<https://doi.org/10.1016/j.marpolbul.2025.117835>.
- Ji, Y., Marian, A.D., Montie, E.W., 2024. Deep-learning-based detection of recreational vessels in an estuarine soundscape in the may river, South Carolina, Usa. *PLoS One* 19, e0302497. <https://doi.org/10.1371/journal.pone.0302497>.
- Joy, R., Tollit, D., Wood, J., MacGillivray, A., Li, Z., Trounce, K., Robinson, O., 2019. Potential benefits of vessel slowdowns on endangered southern resident killer whales. *Front. Mar. Sci.* 6, 344. <https://doi.org/10.3389/fmars.2019.00344>.
- Kaplan, M.B., Mooney, T.A., 2015. Ambient noise and temporal patterns of boat activity in the Us Virgin Islands national park. *Mar. Pollut. Bull.* 98, 221–228. <https://doi.org/10.1016/j.marpolbul.2015.06.047>.
- Keen, E., Hendricks, B., Shine, C., Wray, J., Picard, C.R., Alidina, H.M., 2022. A simulation-based tool for predicting whale-vessel encounter rates. *Ocean Coast. Manag.* 224, 106183. <https://doi.org/10.1016/j.ocecoaman.2022.106183>.
- Lacy, R.C., Williams, R., Ashe, E., Balcomb III, K.C., Brent, L.J., Clark, C.W., Croft, D.P., Giles, D.A., MacDuffee, M., Paquet, P.C., 2017. Evaluating anthropogenic threats to endangered killer whales to inform effective recovery plans. *Sci. Rep.* 7, 14119. <https://doi.org/10.1038/s41598-017-14471-0>.
- Liu, D., Yang, H., Hou, W., Wang, B., 2024. A novel underwater acoustic target recognition method based on mfcc and racnn. *Sensors* 24, 273. <https://doi.org/10.3390/s24010273>.
- MacGillivray, A., De Jong, C., 2021. A reference spectrum model for estimating source levels of marine shipping based on automated identification system data. *Journal of Marine Science and Engineering* 9, 369. <https://doi.org/10.3390/jmse9040369>.
- MacGillivray, A., Stothart, F., Li, Z., Grooms, C., Zykov, M., 2024. Regional 2022 ocean noise contributors in southern resident killer whale habitat: update to the ECHO study on regional 2015 ocean noise contributors, technical report, JASCO applied sciences for innovation centre of transport Canada. <https://open-science.canada.ca/items/5f0c36ba-5a78-4511-a7ca-c8361edcfaf1/full>.
- MacGillivray, A.O., Martin, S.B., Ainslie, M.A., Dolman, J.N., Li, Z., Warner, G.A., 2023. Measuring vessel underwater radiated noise in shallow water. *J. Acoust. Soc. Am.* 153, 1506–1524. <https://doi.org/10.1121/1.50017433>.
- Malinka, C.E., Tollit, D.J., Trounce, K.B., Wood, J.D., 2024. Evaluating the benefits of noise reduction mitigation: The echo program. In: The effects of noise on aquatic life: principles and practical considerations. Springer, pp. 1715–1734. [https://doi.org/10.1007/978-3-031-10417-6\\_100-1](https://doi.org/10.1007/978-3-031-10417-6_100-1).
- Marotte, E., Wright, A.J., Breeze, H., Wingfield, J., Matthews, L.P., Risch, D., Merchant, N.D., Barclay, D., Evers, C., Lawson, J., et al., 2022. Recommended metrics for quantifying underwater noise impacts on North Atlantic right whales. *Mar. Pollut. Bull.* 175, 113361. <https://doi.org/10.1016/j.marpolbul.2022.113361>.
- Mattmüller, R.M., Thomisch, K., Hoffman, J.I., Van Opzeeland, I., 2024. Characterizing offshore polar ocean soundscapes using ecoacoustic intensity and diversity metrics. *R. Soc. Open Sci.* 11, 231917. <https://doi.org/10.1098/rsos.231917/v2/review1>.
- McDonald, M.A., Hildebrand, J.A., Wiggins, S.M., 2006. Increases in deep ocean ambient noise in the northeast pacific west of san nicolas island, California. *J. Acoust. Soc. Am.* 120, 711–718. <https://doi.org/10.1121/1.2216565>.
- McKenna, M.F., Ross, D., Wiggins, S.M., Hildebrand, J.A., 2012. Underwater radiated noise from modern commercial ships. *J. Acoust. Soc. Am.* 131, 92–103. <https://doi.org/10.1121/1.3664100>.
- Merchant, N.D., Pirotta, E., Barton, T.R., Thompson, P.M., 2014. Monitoring ship noise to assess the impact of coastal developments on marine mammals. *Mar. Pollut. Bull.* 78, 85–95. <https://doi.org/10.1016/j.marpolbul.2013.10.058>.
- O. Murphy, R. Fairfield Checko, M. Young, L. Laturun, T.-W. Lin, B. Padovese, R. Joy, Analysis of southern resident killer whale management measures surrounding saturna island, 2023. URL: [https://www.sfu.ca/rjoy/SaturnaAnalysisOfMeasure\\_s.SFU.pdf](https://www.sfu.ca/rjoy/SaturnaAnalysisOfMeasure_s.SFU.pdf). doi: 10.56507/jwul5276.
- O'Hara, P.D., Serra-Sogas, N., McWhinnie, L., Pearce, K., Le Baron, N., O'Hagan, G., Neddoly, A., Marques, T., Canessa, R., 2023. Automated identification system for ships data as a proxy for marine vessel related stressors. *Sci. Total Environ.* 865, 160987. <https://doi.org/10.2139/ssrn.4150582>.
- Peng, C., Zhao, X., Liu, G., 2015. Noise in the sea and its impacts on marine organisms. *Int. J. Environ. Res. Public Health* 12, 12304–12323. <https://doi.org/10.3390/ijerph121012304>.
- Pine, M.K., Hannay, D.E., Inslay, S.J., Halliday, W.D., Juanes, F., 2018. Assessing vessel slowdown for reducing auditory masking for marine mammals and fish of the western Canadian arctic. *Mar. Pollut. Bull.* 135, 290–302. <https://doi.org/10.1016/j.marpolbul.2018.07.031>.
- A. Pollara, A. Sutin, H. Salloum, Passive acoustic methods of small boat detection, tracking and classification, in: 2017 IEEE international symposium on Technologies for Homeland Security (HST), IEEE, 2017, pp. 1–6. doi:<https://doi.org/10.1109/th.s.2017.7943488>.
- Popper, A.N., Hawkins, A.D., 2019. An overview of fish bioacoustics and the impacts of anthropogenic sounds on fishes. *J. Fish Biol.* 94, 692–713. <https://doi.org/10.1111/jfb.13948>.
- Reis, C.D., Padovese, L.R., de Oliveira, M.C., 2019. Automatic detection of vessel signatures in audio recordings with spectral amplitude variation signature. *Methods Ecol. Evol.* 10, 1501–1516. <https://doi.org/10.1111/2041-210x.13245>.
- Robards, M., Silber, G., Adams, J., Arroyo, J., Lorenzini, D., Schwehr, K., Amos, J., 2016. Conservation science and policy applications of the marine vessel automatic identification system (ais)—a review. *Bull. Mar. Sci.* 92, 75–103. <https://doi.org/10.5343/bms.2015.1034>.
- Rolland, R.M., Parks, S.E., Hunt, K.E., Castelleto, M., Corkeron, P.J., Nowacek, D.P., Wasser, S.K., Kraus, S.D., 2012. Evidence that ship noise increases stress in right whales. *Proc. R. Soc. B Biol. Sci.* 279, 2363–2368. <https://doi.org/10.1063/pt.5.025868>.
- Ross, D., 2013. Mechanics of underwater noise. Elsevier. <https://doi.org/10.1016/c2013-0-02819-8>.
- Serra-Sogas, N., O'Hara, P.D., Pearce, K., Smallshaw, L., Canessa, R., 2021. Using aerial surveys to fill gaps in ais vessel traffic data to inform threat assessments, vessel management and planning. *Mar. Policy* 133, 104765. <https://doi.org/10.1016/j.marpol.2021.104765>.
- Siddagangaiah, S., Li, Y., Guo, X., Chen, X., Zhang, Q., Yang, K., Yang, Y., 2016. A complexity-based approach for the detection of weak signals in ocean ambient noise. *Entropy* 18, 101. <https://doi.org/10.3390/e18030101>.

- Simard, P., Wall, K.R., Mann, D.A., Wall, C.C., Stallings, C.D., 2016. Quantification of boat visitation rates at artificial and natural reefs in the eastern gulf of Mexico using acoustic recorders. *PLoS One* 11, e0160695. <https://doi.org/10.1371/journal.pone.0160695>.
- Slabbekoorn, H., Bouton, N., van Opzeeland, I., Coers, A., ten Cate, C., Popper, A.N., 2010. A noisy spring: the impact of globally rising underwater sound levels on fish. *Trends Ecol. Evol.* 25, 419–427. <https://doi.org/10.1016/j.tree.2010.04.005>.
- Sorensen, E., Ou, H.H., Zurk, L.M., Siderius, M., 2010. Passive acoustic sensing for detection of small vessels. In: *OCEANS 2010 MTS/IEEE. IEEE, SEATTLE*, pp. 1–8. <https://doi.org/10.1109/oceans.2010.5664542>.
- Southall, B.L., Finneran, J.J., Reichmuth, C., Nachtigall, P.E., Ketten, D.R., Bowles, A.E., Ellison, W.T., Nowacek, D.P., Tyack, P.L., 2019. Marine mammal noise exposure criteria: updated scientific recommendations for residual hearing effects. *Aquat. Mamm.* 45, 125–232. <https://doi.org/10.1578/am.45.2.2019.125>.
- Tasker, M., Amundin, M., Andre, M., Hawkins, A., Lang, W., Merck, T., Scholik-Schlomer, A., Teilmann, J., Thomsen, F., Werner, S., et al., 2010. Underwater noise and other forms of energy. Report No. EUR 24341, 2010. <https://doi.org/10.2788/87079>.
- Tennessen, J.B., Holt, M.M., Wright, B.M., Hanson, M.B., Emmons, C.K., Giles, D.A., Hogan, J.T., Thornton, S.J., Deecke, V.B., 2024. Males miss and females forgo: auditory masking from vessel noise impairs foraging efficiency and success in killer whales. *Glob. Chang. Biol.* 30, e17490. <https://doi.org/10.1111/gcb.17490>.
- Thornton, S.J., Toews, S., Burnham, R., Konrad, C.M., Stredulinsky, E., Gavrilchuk, K., Thupaki, P., Vagle, S., 2022. Areas of elevated risk for vessel-related physical and acoustic impacts in southern resident killer whale (*Orcinus orca*) critical habitat. Canadian Science Advisory Secretariat (CSAS). <https://doi.org/10.56507/jwul5276>.
- van der Knaap, I., Ashe, E., Hannay, D., Bergman, A.G., Nielsen, K.A., Lo, C.F., Williams, R., 2022. Behavioural responses of wild Pacific salmon and herring to boat noise. *Mar. Pollut. Bull.* 174, 113257. <https://doi.org/10.1016/j.marpolbul.2021.113257>.
- Veirs, S., Veirs, V., Wood, J.D., 2016. Ship noise extends to frequencies used for echolocation by endangered killer whales. *PeerJ* 4, e1657. <https://doi.org/10.7287/peerj.1657v0.1/reviews/1>.
- Veirs, V., Veirs, S., 2005. Average levels and power spectra of ambient sound in the habitat of southern resident orcas. NMFS Contract Report No. AB133F05SE6681, 16p. <https://doi.org/10.1016/b978-0-12-821139-7.00185-9>.
- Vieira, M., Amorim, M.C.P., Sundelöf, A., Prista, N., Fonseca, P.J., 2020. Underwater noise recognition of marine vessels passages: two case studies using hidden Markov models. *ICES J. Mar. Sci.* 77, 2157–2170. <https://doi.org/10.1093/icesjms/fsz194>.
- Wang, J., Chen, Z., 2019. Feature extraction of ship-radiated noise based on intrinsic time-scale decomposition and a statistical complexity measure. *Entropy* 21, 1079. <https://doi.org/10.3390/e21111079>.
- Wenz, G.M., 1962. Acoustic ambient noise in the ocean: spectra and sources. *J. Acoust. Soc. Am.* 34, 1936–1956. <https://doi.org/10.1121/1.1909155>.
- Williams, R., Erbe, C., Ashe, E., Beerman, A., Smith, J., 2014. Severity of killer whale behavioral responses to ship noise: a dose–response study. *Mar. Pollut. Bull.* 79, 254–260. <https://doi.org/10.1016/j.marpolbul.2013.12.004>.
- Wilson, L., Pine, M.K., Radford, C.A., 2022. Small recreational boats: a ubiquitous source of sound pollution in shallow coastal habitats. *Mar. Pollut. Bull.* 174, 113295. <https://doi.org/10.1016/j.marpolbul.2021.113295>.
- Wright, A.J., Soto, N.A., Baldwin, A.L., Bateson, M., Beale, C.M., Clark, C., Deak, T., Edwards, E.F., Fernández, A., Godinho, A., et al., 2007. Do marine mammals experience stress related to anthropogenic noise? *Int. J. Comp. Psychol.* 20. <https://doi.org/10.46867/ijcp.2007.20.02.01>.
- ZoBell, V.M., Hildebrand, J.A., Frasier, K.E., 2024. Comparing pre-industrial and modern ocean noise levels in the Santa Barbara channel. *Mar. Pollut. Bull.* 202, 116379. <https://doi.org/10.1016/j.marpolbul.2024.116379>.